PE&RS

February 2025 Volume 91, Number 2

PHOTOGRAMMETRIC ENGINEERING & REMOTE SENSING

The official journal for imaging and geospatial information science and technology

GEO WEEK

Scan for Committee Meeting schedule and Zoom links

ASPRS Committee Meetings

ASPRS Division and Committee Meetings held during Geo Week are open to the public and do not require a conference badge or ASPRS membership to attend. These meetings are intended to:

1. Provide an opportunity for thought leaders to get together face-to-face to discuss important ASPRS-sponsored initiatives that feed into our overarching mission, such as :
   - development of standards and best-practice guidelines
   - development of education materials to facilitate the implementation of these standards and guidelines
   - develop strategies to further broad implementation of these standards and guidelines across the industry/profession
   - identify themes of interest to the readership of our monthly journal
   - identify potential authors of journal articles on these topics
   - support our professional certification program, particularly with respect to exam content
2. Host invited presentations on focused topics that are of keen interest to smaller groups of technically-focused individuals.
3. Provide an opportunity for conference attendees who are not ASPRS members to learn more about the Society and the benefits of individual membership.

Monday, February 10

Student Advisory Council	Bluebird 3F	8:30–9am
Higher Logic Microsite Help Session	Bluebird 3F	9–10:30am
Photogrammetric Applications Division	Bluebird 3E	9–11:30am
Evaluation for Certification Committee	Bluebird 3F	12–1:00pm
UAS Division	Bluebird 3E	12:30–1pm
GIS Division Committee	Bluebird 3F	1–1:30pm
Early Career Professionals Council	Bluebird 3E	1–1:30pm
Photogrammetric Applications Division	Bluebird 3E	3:30–4:30pm
Heartland Region	Bluebird 3F	4:30– 5pm

Tuesday, February 11

Bathymetric Lidar Working Group	Bluebird 3E	10–11am
Remote Sensing Applications Division	Bluebird 3E	11:30–12:00pm
Awards and Scholarship Committee	Bluebird 3F	1–2pm
Rocky Mountain Region	Bluebird 3E	1–2pm
Data Preservation and Archiving Committee	Bluebird 3F	2–3pm
Standards Committee	Bluebird 3E	2–3pm
Lidar Division	Bluebird 3F	3:30–4:30pm
Primary Data Acquisition Division	Bluebird 3E	3:30–4:30pm

Wednesday, February 12

NSRS Modernization Working Group	Bluebird 3F	9–10am
LAS Working Group	Bluebird 3E	1–2pm

Awards Ceremony

Tuesday, February 11 | Bluebird 3C | 4:30–5:30pm
Sponsored by Woolpert

Awards include Professional Awards, Society Awards, Installations of Officers, and Outstanding Paper Awards. We will have drawings throughout the ceremony for your chance to win a prize! We look forward to celebrating with you!

Future Leaders Hub

The posters and the presentation recordings of the 2024 ASPRS GeoChallenge as well as posters of the ASPRS Student Chapters will be showcased in the **Future Leaders Hub** in the Exhibit Hall.

asprs THE IMAGING & GEOSPATIAL INFORMATION SOCIETY

COME VISIT ASPRS IN **BOOTH 1533**

my.asprs.org/2025Conference

asprs THE IMAGING & GEOSPATIAL INFORMATION SOCIETY

ASPRS MEMBERSHIP

Joining ASPRS is a great way to boost your resume and learn valuable life lessons

WHY GET INVOLVED WITH ASPRS?

- Develop leadership skills
- Experience working on a team
- Gain valuable soft skills
- Network
- Learn about yourself
- Have fun!

Scholarships

The many ASPRS scholarships are only available to student members

Certification

The ASPRS certification program for mapping scientists, photogrammetrists and technologists is the only fully Accredited certification program in the geospatial sciences

Continuing Education

Earn professional development hours and CEUs by attending workshops at our conferences and on-line as well as our monthly on-line geobytes series

PE&RS

Our monthly journal, is packed with informative and timely articles designed to keep you abreast of current developments in your field. Now available in e-format.

Get Connected

facebook.com/ASPRS.org

linkedin.com/company/asprs/about/

twitter.com/ASPRSorg

youtube.com/user/ASPRS

Image and text courtesy the ASPRS Florida Region

asprs FLORIDA REGION THE IMAGING & GEOSPATIAL INFORMATION SOCIETY

PE&RS

PHOTOGRAMMETRIC ENGINEERING & REMOTE SENSING

The official journal for imaging and geospatial information science and technology

February 2025 Volume 91 Number 2

COLUMNS

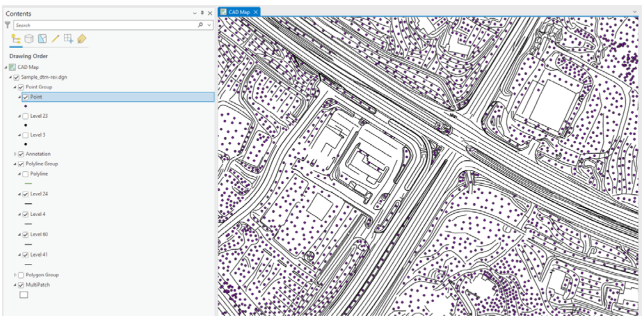

ANNOUNCEMENTS

Dr. Jie Shan

DEPARTMENTS

See the Cover Description on Page 68

COVER DESCRIPTION

Like other parts of the Canadian Shield, water is omnipresent in the Mauricie region of Quebec. Numerous lakes, large and small, dot the surface—a byproduct of the glaciers that carved depressions into the region's igneous bedrock during the most recent ice age.

However, people also played a role in shaping the region&rquo;s waterways when they created Réservoir Gouin, the sprawling many-armed lake shown in this satellite image. The scene was acquired by the OLI (Operational Land Imager) on Landsat 8 on October 17, 2023. Dark patches northwest of the reservoir are recent burned areas; brown and yellow areas to the east have been logged.

Construction of the Gouin dam began in 1916 to regulate the flow of the Saint-Maurice River and make it easier to float wood to pulp and paper mills downstream. After the concrete structure—measuring 26 meters (85 feet) high and 502 meters (1,647 feet) long—was finished, it transformed the network of lakes and river valleys upstream into what was then the world's largest reservoir. It also meant that Obedjiwan (also spelled Opitciwan), an Atikamekw village on the north shore of the new reservoir, had to move to higher ground.

Before the dam's construction, the flow of the Saint-Maurice River varied sharply from one season to the next. In 1913, for instance, it fluctuated between 170 cubic meters per second in the summer and 5,700 cubic meters per second during the spring flood, according to Hydro Québec.

The dam ultimately curtailed such swings, but the reservoir still sees seasonal variations. In winter, managers lower water levels to make room for spring snowmelt and summer rains, and they allow water levels to peak in the late summer or fall.

Such seasonal variations in the water level are observable from space. Gouin is among more than 300 lakes and reservoirs that NASA scientists monitor using data collected by radar altimeters on several satellites, including Jason-2, Jason-3, and Sentinel-6 Michael Freilich.

The project, based at NASA's Goddard Space Flight Center, posts new water height measurements of the reservoir every two weeks. The reservoir's water levels typically drop a few meters in the winter and have trended upward by a few meters overall since the 1990s, the satellite observations show.

References

Community Stories (2024) Opitciwan in 1933. Accessed December 13, 2024.

Community Stories (2020) A Source of Sustenance. Accessed December 13, 2024.

Hydro Québec (2024) The Guardian of the Rivière Saint-Maurice. Accessed December 13, 2024.

NASA (2024) Global Water Measurements. Accessed December 13, 2024.

Opitciwan Atikamekw Council Welcome. Accessed December 13, 2024.

Québec (2024) Geological Map of Québec. Accessed December 13, 2024.

NASA Earth Observatory image by Michala Garrison, using Landsat data from the U.S. Geological Survey. Story by Adam Voiland.

This image record originally appeared on the Earth Observatory. Visit https://earthobservatory.nasa.gov/images/153683/the-many-arms-of-reservoir-gouin to view the full, original record.

asprs

THE IMAGING & GEOSPATIAL INFORMATION SOCIETY

PHOTOGRAMMETRIC ENGINEERING & REMOTE SENSING

Journal Staff

Publisher ASPRS
Editor-In-Chief Rongjun Qin
Director of Publications Rae Kelley
Electronic Publications Manager/Graphic Artist Matthew Austin

Photogrammetric Engineering & Remote Sensing is the official journal of the American Society for Photogrammetry and Remote Sensing. It is devoted to the exchange of ideas and information about the applications of photogrammetry, remote sensing, and geographic information systems. The technical activities of the Society are conducted through the following Technical Divisions: Geographic Information Systems, Photogrammetric Applications, Lidar, Primary Data Acquisition, Professional Practice, Remote Sensing Applications, and Unmanned Autonomous Systems. Additional information on the functioning of the Technical Divisions and the Society can be found in the Yearbook issue of PE&RS.

All written correspondence should be directed to the American Society for Photogrammetry and Remote Sensing, PO Box 14713, Baton Rouge, LA 70898, including general inquiries, memberships, subscriptions, business and editorial matters, address changes, manuscripts for publication, advertising, back issues, and publications. The telephone number of the Society Headquarters is 225-408-4747; the fax number is 225-408-4422; the web address is www.asprs.org.

PE&RS. *PE&RS* (ISSN0099-1112) is published monthly by the American Society for Photogrammetry and Remote Sensing, 8550 United Plaza Blvd, Suite 1001, Baton Rouge, Louisiana 70809. Periodical postage paid at Bethesda, Maryland and at additional mailing offices.

SUBSCRIPTION. *PE&RS* is available as an e-Subscription (single-site and multi-site licenses) and an e-Subscription with print add-on (single-site license only). *PE&RS* subscriptions are on a calendar-year, beginning in January and ending in December.

The rate for a single-site e-Subscription for the USA/Non-USA is $1040 USD, for Canadian* is $1092 USD.

The rate for a multi-site e-Subscription for the USA/Non-USA is $1040 USD plus $250 USD for each additional license, for Canadian* is $1092 USD plus $263 for each additional license.

The rate for e-Subscription with print add-on for the USA is $1546 USD, for Canadian* is $1637 USD, and for Non-USA is $1596 USD.

*Note: Subscription prices for Canada includes 5% of the total amount for Canada's Goods and Services Tax (GST #135123065). **PLEASE NOTE: All Subscription Agencies receive a 20.00 USD discount**.

POSTMASTER. Send address changes to PE&RS, ASPRS, PO Box 14713, Baton Rouge, LA 70898. CDN CPM #(40020812).

MEMBERSHIP. Membership is open to any person actively engaged in the practice of photogrammetry, photointerpretation, remote sensing and geographic information systems; or who by means of education or profession is interested in the application or development of these arts and sciences. Membership is for one year, with renewal based on the anniversary date of the month joined. Membership Dues include a 12-month electronic subscription to *PE&RS*. Annual Individual Membership dues are $175.00 USD and Student Membership dues are $50.00 USD. A tax of 5% for Canada's Goods and Service Tax (GST #135123065) is applied to all members residing in Canada.

ANNOUNCEMENTS

GeoCue (www.geocue.com), is pleased to announce the addition of Epotronic as its latest distributor in Germany. Based in Düsseldorf, Epotronic specializes in the commercial distribution and use of surveying drones, industrial drones, sensors, and laser scanners for surveying and inspection purposes.

Samuel Flick and the Epotronic team at Intergeo 2024 (image courtesy GeoCue)

"We are excited to welcome Epotronic to our network of distributors," said Samuel Flick, European Sales Manager at GeoCue. "Their expertise in drone technology and commitment to providing tailored solutions sync with our goal to deliver best-in-class hardware and software to our customers."

Epotronic is well known for offering drone and sensor solutions that are tailored to meet the individual requirements of their clients. With an extensive network and years of experience, they now bring GeoCue's TrueView 3D Imaging Systems (https://geocue.com/sensors/drone-lidar/) and LP360 (https://www.lp360.com/) software into its extensive catalog of equipment, surveying supplies, and software solutions. This partnership aims to empower Epotronic's customers with efficient and accurate surveying tools that seamlessly integrate into their workflow, enhancing their overall productivity.

"Partnering with GeoCue allows us to fulfill our customers' needs with precise, reliable, and consistent surveying results at fair pricing for years to come," said Tobias Wentzler, CEO of Epotronic GmbH. "GeoCue's TrueView LiDAR products and LP360 software are best-in-class, and we're confident that this collaboration will bring significant value to surveying and construction companies, government entities, and universities across Germany."

Epotronic's decision to become a TrueView and LP360 provider was driven by GeoCue's reputation for delivering high-performance products backed by a trusted and experienced team. This partnership is expected to enhance the capabilities of professionals in the surveying and inspection industries by providing access to cutting-edge technology and comprehensive support services.

Epotronic's expertise goes beyond technology. The company provides comprehensive training and customer project support, ensuring businesses can seamlessly integrate advanced drone and sensor technology into their operations with minimal investment risk.

Epotronic's addition to GeoCue's global distribution network marks another step in expanding access to transformative lidar and geospatial solutions worldwide.

After a competitive bid process, the Indiana Geographic Information Office (IGIO) has tasked **Woolpert** (www.woolpert.com), with acquiring aerial orthoimagery and lidar data for the state of Indiana. Collected as a part of the IGIO's Imagery (https://imagery.gio.in.gov/) and Elevation Programs (https://elevation.gio.in.gov/), these data will support economic development, infrastructure, conservation, and emergency response planning needs throughout the state.

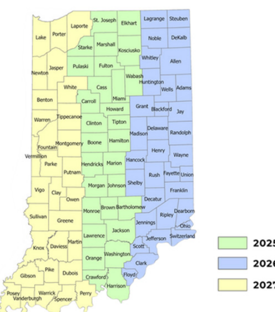

Courtesy IGIO's Imagery Program

Under the contract, Woolpert will simultaneously acquire over 37,000 square miles of four-band, 6-inch resolution digital orthoimagery and Quality Level 1 lidar over a three-year period from 2025-2027. Woolpert also will acquire approximately 120 square miles of 3-inch resolution digital orthoimagery and QL1 lidar along the coast of Lake Michigan each year through 2028 in support of the Indiana Department of Natural Resources' Lake Michigan Coastal Program (https://www.in.gov/dnr/lake-michigan-coastal-program/). QL1 data are delivered at 25 points per square meter.

The data will be available at no cost for the public to download or stream through the IGIO website (https://www.in.gov/gis/) and IndianaMap (https://www.indianamap.org/). State and local government agencies can obtain additional services and products, including enhanced digital orthoimagery, lidar, and derivative datasets, through the state's collective buy-up program.

Woolpert Project Manager Matt Worthy said that local governments rely on geospatial data for countless processes. The data serves as a base map for a range of applications, including planning, assessment, modelling, and research.

"The usefulness of the state's orthoimagery and lidar data is virtually endless," Worthy said. "In addition to the classic use cases of the base imagery and elevation data, we've already begun receiving requests for derivative products such as building footprints, impervious surfaces, elevation-derived hydrography, the list goes on. The excitement surrounding the program is palpable from the metropolitan government coalitions, down to the smallest rural counties and municipalities. It's rewarding to explain Woolpert's solution to others and watch their wheels start turning as they connect our data to projects that they've wanted to undertake but maybe haven't due to previous technological or cost considerations."

Woolpert Program Director Brian Stevens noted the growth and sophistication of Indiana's statewide imagery and lidar programs.

"When I first started my career at Woolpert and working with several Indiana counties, we primarily collected and processed black-and-white aerial imagery to produce ortho-imagery and manually derived derivative products," Stevens said. "Now, with the technology being implemented today by the state, including high point density lidar and co-collected aerial imagery, Indiana is leading the way and serves as a model for the rest of the country."

The contract is underway. Data acquisition is expected to begin this spring.

L3Harris Technologies (www.l3harris.com), has received a contract from the U.S. Space Force's Space Systems Command to design concepts for Phase 0 of the Resilient Global Positioning System (R-GPS) program.

The R-GPS program is a procurement of cost-effective small satellites that will augment the existing 31-satellite GPS constellation providing resilience to military and civil GPS users. Space Force plans to produce and launch up to eight satellites to address jamming, spoofing and more permanent disruptions.

"We are answering the call to protect and defend national security interests by developing and deploying reliable and robust GPS technologies crucial to the warfighter and the global populace," said Ed Zoiss, President, Space and Airborne Systems, L3Harris. "We will leverage our five decades of experience as a key mission partner providing GPS to deliver a more resilient Positioning, Navigation and Timing (PNT) infrastructure."

L3Harris is the only company to provide navigation technology for every U.S. GPS satellite ever launched, in addition to designing and building critical elements of the control segment, monitor station receivers and user equipment. This mature technology provides the foundation of the L3Harris R-GPS solution.

L3Harris' investment in transformational PNT technology uses commercial form factors and interfaces for a modular, scalable solution supporting Space Force needs. L3Harris is also collaborating with the Space Force as the prime contractor on the experimental Navigation Technology Satellite-3 program to develop cutting-edge technology and deliver on accelerated development timelines.

The U.S. Geological Survey (www.usgs.gov), has tasked **Woolpert** (www.woolpert.com), with collecting 28,043 square miles of topographic Quality Level 1 lidar data and providing ground control survey across western Arkansas in support of the 3D Elevation Program (3DEP) and The National Map.

The data will be merged with 24,533 square miles of QL1 lidar data currently being collected across eastern Arkansas under a separate contract awarded to Woolpert last year.

3DEP, led by the USGS National Geospatial Program, offers the nation's first baseline of seamless, high-resolution topographic elevation data, which is then incorporated into The National Map. The data is free and publicly available to local, state, and national agencies. It is used to inform decisions that impact the immediate safety of life, property, and the environment, and is critical to effective, long-term infrastructure planning.

Under this second task order, Woolpert will fly 1,048 flight lines and collect approximately 450 ground control survey points. The aerial lidar data will be collected this winter and is expected to be delivered in summer 2026.

"This new lidar will have a higher level of point density, allowing for preliminary designs and providing topographic survey that engineers can use for a variety of projects, including levelling farm fields, building and improving levees, construction of roadways, and stormwater engineering," Woolpert Program Director Sam Moffat said. "This data will also enable the state to assist in managing its natural resources and will be particularly useful for applications like forest inventory, biodiversity assessment, watershed analysis, geological mapping, and monitoring environmental changes, providing crucial data for informed decision-making in conservation and resource management strategies."

The contract is underway.

CALENDAR

- 3-8 August, IEEE International Geoscience and Remote Sensing Symposium, Brisbane, Australia; https://2025.ieeeigarss.org.
- 16-22 August, **32nd International Cartographic Conference**, Vancouver, Canada; https://cartogis.org/usnc-ica.

GIS

Tips & Tricks

By Al Karlin, Ph.D., CSM-L, GISP

Picking a GIS file format

INTRODUCTION

In 2025, Esri's Arc/Info™ is so far in the rearview mirror, that ArcGIS Pro 3.X does not provide support or a conversion tool for, what was called, "a coverage"; the Esri proprietary GIS standard file format that incorporated the geometry (arcs), the feature attributes (info), the "tics", and several other supporting feature-related indexing files into a single file folder. To say that this format was cumbersome would be an understatement.

So, in the early 1990s, Esri introduced the "shapefile" format, actually three files, a .SHP file containing the geometry, a .DBF, DBase 4™, file containing the feature attributes, and a .SHX file, an index file, as the native digital vector data format for their new ArcView software product. The shapefile became so popular among GIS practitioners, that in 1998, Esri released the format. Today, the shapefile remains proprietary, but the technical specifications are open and can be used freely. Most, if not all, GIS software can import and display the Esri shapefile.

The Esri shapefile, however, has several limitations. As a collection of 8-bit files, shapefiles cannot exceed 2 gigabytes in size. The file size limits the file to approximately 70 million point features; certainly not sufficient for lidar data storage, and the number of lines and/or polygons that can be stored is dependent on the number of vertices. Field names for attributes, cannot exceed 10 characters and can contain only letters, numbers and underscores. Precision issues arise when importing/exporting 8-bit shapefiles into/out of 16-bit geodatabases. Shapefiles also cannot store Time and Data in the same files and NULL values are stored as zero. The list of limitations goes on and on. Finally, as shapefiles require large amounts of storage, other GIS formats and in particular interchange formats become important. This month, I'll focus on three GIS data formats that are commonly encountered in the GIS world.

TIP 1: Using AutoCAD™ and MicroStation™ files in the Esri ArcGIS Pro environment

Computer-aided Design (CAD) files are vector representations of design plans and specifications usually intended to be printed on 24" x 36" sheets of paper. CAD files typically contain lines, points, and annotation, but as the file was intended to be printed, there would be no need for georeferencing and CAD drafters generally place the origin (i.e. start their drawing) at an arbitrary coordinate in the CAD coordinate space, usually at 0,0 (or sometimes at 5000,5000). In the real world, that would place the origin somewhere on the equator in the Atlantic Ocean! In last month's *PE&RS* GIS Tips & Tricks column (*PE&RS*, October 2024), Delaney Resweber and I discussed some tips for georeferencing CAD files. So, the first thing that a GIS analyst needs to do is to confirm the coordinate reference system of the CAD file and "georeference" the file as needed.

Among the most commonly used CAD programs are AutoDesk AutoCAD™ and Bentley Microstation™. It is fairly common for a GIS analyst to be asked to incorporate either one of these CAD files into a GIS project. AutoCAD™ files will be either (1) drawing files (.DWG) or (2) ASCII files specifically designed for interchange among software programs (.DXF), while Microstation™ files will generally be design files (.DGN). In either case, ArcGIS Pro will open the CAD file's database, and show groups of points, lines, polygons, and the annotation as in Figure 1 below.

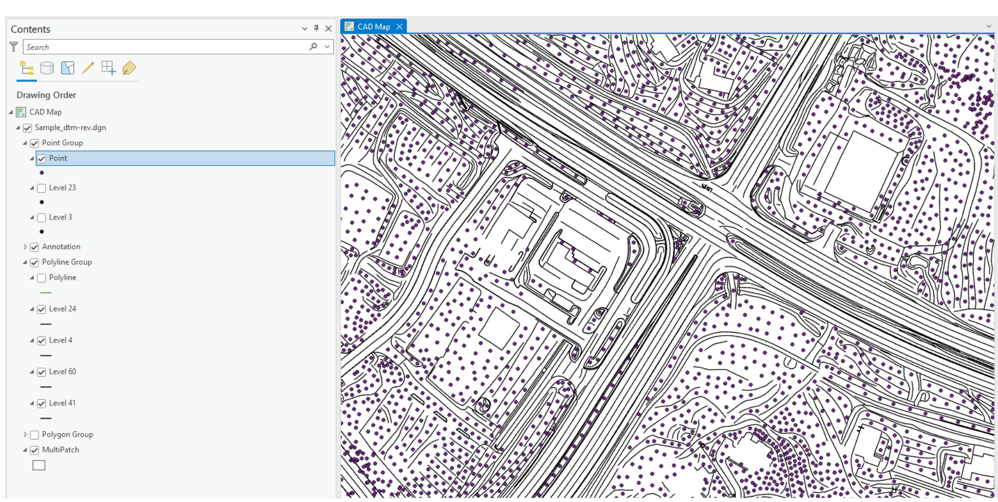

Figure 1. A MicroStation™ design file in ArcGIS Pro 3.3.

Selecting any individual feature, as in the Point feature selected in Figure 1, and clicking on the Layer Feature on the ribbon will start the CAD Data options as in Figure 2. Using the tools on this ribbon, you can control the Alignment (= georeferencing) of the feature, as well as perform several GIS functions (Export, Copy, etc.).

In this case (Figure 1), I am showing a MicroStation™ .DGN file, but AutoCAD™ files behave in a similar manner. For more information, here is a link to the Esri help (https://pro.arcgis.com/en/pro-app/latest/help/data/cad/cad-data-in-arcgis-pro.htm) and there are several YouTube tutorials available (https://www.youtube.com/watch?v=QTW3_k7jiok) for viewing.

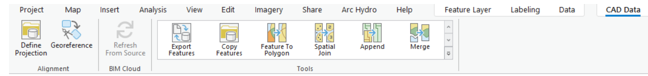

Figure 2. The CAD Data option ribbon in ArcGIS Pro.

TIP #2: Using Keyhole Markup Language (KML) in ArcGIS Pro

Another common file format is Keyhole Markup Language (KML) made popular by Google Earth™. KML originated in the early 2000s by Keyhole, Inc. Google™ acquired Keyhole in 2004 and incorporated KML into Google Earth™. This Extensible Markup (XML)-based language is very compact and can represent points, lines, polygons and annotation in a georeferenced framework. KML and the compressed form, Keyhole Markup Language Zipped (KMZ) is easily transported on USB drives or sent over e-mail, as most files are under 1 megabyte.

ArcGIS Pro cannot ingest or display KML files directly, however, there are tools in the Data Conversion | KML toolset to convert KML to Layers (and Layers to KML) for using in ArcGIS Pro (Figure 3).

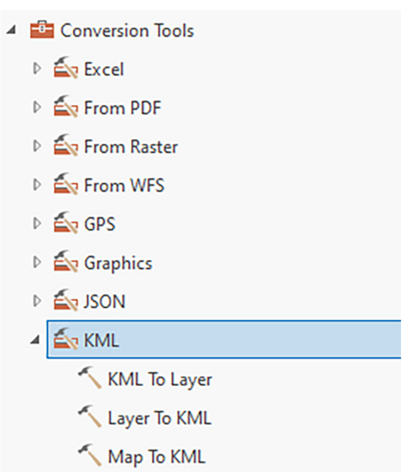

Figure 3. The Data Conversion Toolbox showing the KML Toolset in ArcGIS Pro.

Double-click to open the KML to Layer dialog box (Figure 4), and fill-in the parameters with (1) the KML (or KMZ) file to convert, (2) a folder to hold the layer(s), and (3) a name for the layer(s), and "Run" the tool.

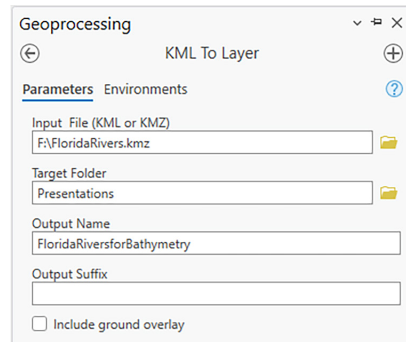

Figure 4. The KML (KMZ) to layer dialog box.

In this case, I imported a KMZ file that contained 4 polygons representing areas around 4 rivers in Florida for hydrographic survey. Once the KMZ file was converted to a layer file, I changed the symbology to blue outlined polygons and display the attribute table in Figure 5.

For more information on creating KML/KMZ files on Google Earth, see: https://apollomapping.com/how-to/creating-kmz-file-google-earth, and for more information on importing KML/KMZ files into ArcGIS Pro, see: https://pro.arcgis.com/en/pro-app/latest/tool-reference/conversion/kml-to-layer.htm.

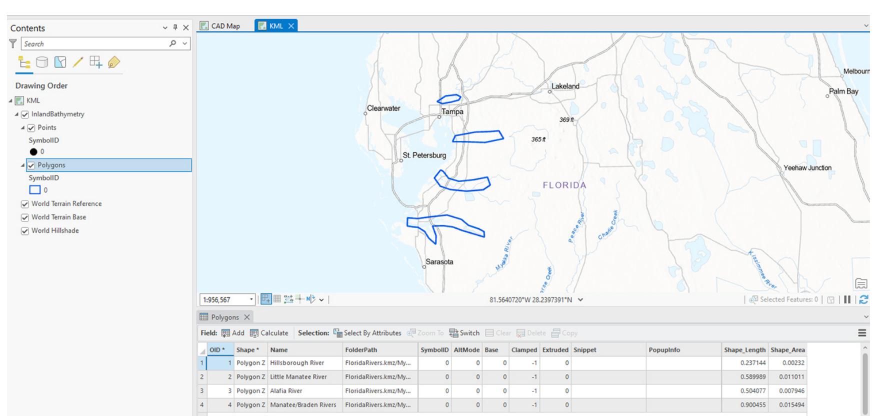

Figure 5. ArcGIS Pro displaying the layer resulting from converting the KML/KMZ file. Note that the file is georeferenced and complete with non-spatial attributes.

TIP #3: Using JSON (GeoJSON) files in ArcGIS Pro

The GeoJSON file format is an open format designed for representing simple (point, line, polygon) geographic features, as well as, multiparts of these features along with non-spatial attributes. The file format is maintained by an Internet Engineering Task Force of developers who released the format in August 2016. Since then, the format has been widely accepted as an open, interchange GIS format. Unfortunately, as an open format, several “flavors” have evolved and not all are immediately convertible for viewing in ArcGIS Pro (see GIS Tips & Tricks, November 2024).

With that, ArcGIS Pro provides conversion tools in the Data Conversion | JSON toolset for conversion to and from the JSON file format (Figure 6). For this example, I am using a GeoJSON file containing the point locations of Agricultural Inspection Stations in Florida. The GeoJSON file is 7KB in size and contains 23 point features. The converted shapefile, seen in Figure 8, is 23 KB, requiring three times the storage!

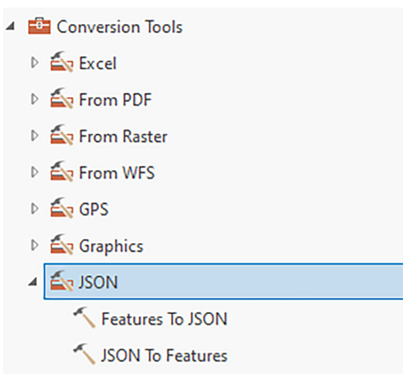

Figure 6. The JSON conversion tools in the ArcGIS Pro Conversion Tools Toolbox.

Use the Data Conversion | JSON | JSON to Feature tool (Figure 6) to open the dialog box (Figure 7), specify the Input JSON or GeoJSON file (in this case a GeoJSON), and the Output Feature Class (the default is a shapefile, but you can put the feature class into a Geodatabase), specify the Geometry Type (in this case as a Point) and run the tool. NOTE: There are no Environmental Parameters to set.

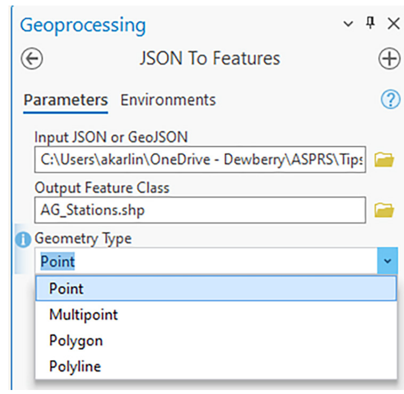

Figure 7. The JSON to Feature dialog box. Be careful to set the proper Geometry Type for the output as the default is “Polygon”.

For more information on converting JSON/GeoJSON files visit the GeoJSON homepage at: https://geojson.org/ or the Esri Help at: JSON To Features (Conversion)—ArcGIS Pro | Documentation (https://pro.arcgis.com/en/pro-app/3.1/tool-reference/conversion/json-to-features.htm)

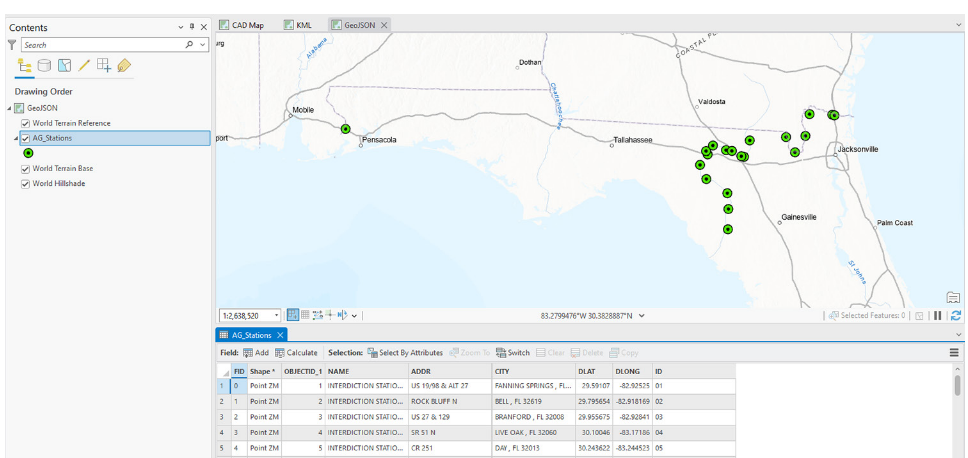

Figure 8. ArcGIS Pro displaying the shapefile resulting from the conversion of the GeoJSON file. Note the file is georeferenced and complete with non-spatial attributes.

TIP #4: For QGIS users – Importing multiple GIS formats into QGIS is generally easier than importing files into ArcGIS, but not always

1. For CAD files, the file needs to be converted to a vector format that QGIS recognizes, and unfortunately, QGIS does not recognize MicroStation™ .DGN files or AutoCAD™ .DWG files. However, the GRASS plug-in does provide a tool in the Vector folder, the v.in.dxf to import an ASCII CAD Exchange file (.DXF),
2. For KML/KMZ files, just drag and drop the file onto the canvas, QGIS will respond with a message (Figure 9) asking which features in the KML/KMZ file to import, select the features and press “add layers” to add the data top your canvas, and

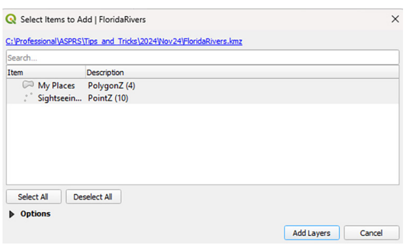

Figure 9. QGIS KML/KMZ import dialog box.

4. For JSON/GeoJSON files, just drag and drop the file onto the canvas and QGIS does the rest!

Send your questions, comments, and tips to GISTT@ASPRS.org.

Al Karlin, Ph.D., CMS-L, GISP is with Dewberry’s Geospatial and Technology Services group in Tampa, FL. As a senior geospatial scientist, Al works with all aspects of lidar, remote sensing, photogrammetry, and GIS-related projects.

ASPRS Directory

Membership/*PE&RS* Subscription
office@asprs.org

Conferences
programs@asprs.org

Certification
applications@asprs.org

Calendar
calendar@asprs.org

ASPRS Bookstore
office@asprs.org

ASPRS Foundation
foundation@asprs.org

ASPRS Board of Directors
asprsboard@asprs.org

Student Advisory Council
sac@asprs.org

Early-Career Professionals Council
ecpc@asprs.org

Region Officers Council
roc@asprs.org

Sustaining Members Council
smc@asprs.org

Technical Division Directors Council
tddc@asprs.org

Mailing Address
PO Box 14713
Baton Rouge, LA 70898
225-408-4747, 225-408-4422 (fax)
www.asprs.org

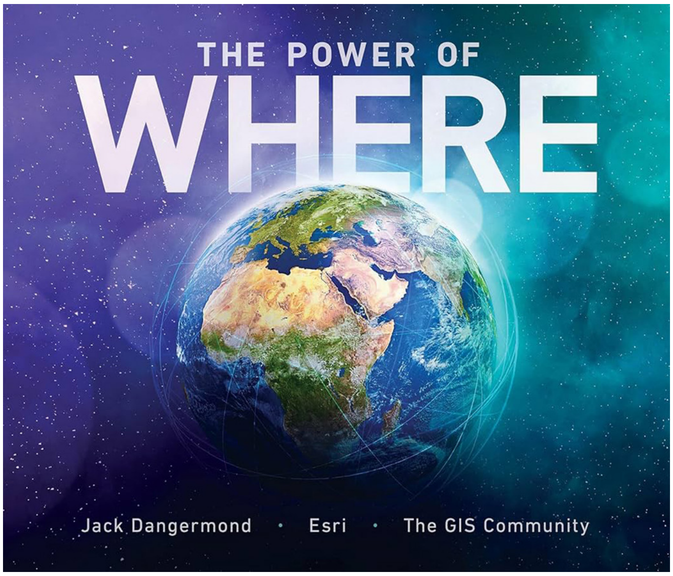

The Power of Where: A Geographic Approach to the World's Greatest Challenges

Jack Dangermond. xxv+274 pages; full color throughout; approximately 600 maps, photos and illustrations. 2024. Esri Press. Print ISBN10: 1589486064; Print ISBN13: 9781589486065; eBook ISBN13: 9781589486072..

Reviewed by Demetrio P. Zourarakis, PhD, GISP, CMS (GIS/LIS, RS, Lidar); Adjunct Assistant Professor, University of Kentucky, Martin-Gatton CAFE; Visiting Lecturer, Kentucky State University, CAHNR

Among other things, Mr. Dangermond's excellent book reads part atlas, part textbook on modern geography, part primer on Geographic Information Systems (GIS), part autobiography, and part collection of multidisciplinary lesson plans. Primarily, it cements the author's legacy as co-founder and rightful leader of a movement which has geography and attendant sciences as its engine and GIS as its vehicle. In essence, this transformative work also constitutes the author's loudest call of duty yet to each and every one of us who is willing to answer his exhortation: observe our world - our planet and the issues it faces, from an endless number of points of view and perspectives, brought about by the power of GIS and geospatial sciences and technologies.

The book's subject matter is solidly encapsulated in its subtitle: "A Geographic Approach to the World's Greatest Challenges." Thus, the book design revolves around a comprehensive distillation of virtually every aspect of human activity, viewed against a backdrop of human- and nature-driven changes to the planet's systems. By no means a catalogue of present-day tribulations and ills, the book offers hope, and a bright outlook, supported by a wealth of effective tools, exploring and exemplifying possible avenues for collaborative amelioration and remediation going forward. Paradigmatically, Mr. Dangermond's life history deeply embodies the evolution of the "power of where" as he puts it, emphasizing the necessary and constant presence of human dimensions, both person-centered and community-centered — in every aspect of geographic knowledge, and by extension of GIS.

This highly dynamic, versatile and thoughtfully constructed book constitutes yet another step in the author's multi-faceted journey as founder of a movement, mentor of countless generations of professionals, and in his role as tireless and perennial tour guide of GIS to a world audience.

The chapters in this book are sandwiched between an impressive *Foreword* (pp. vii) and no less impressive acknowledgements and credits. As a hats-off to map-making, there is a *Beginnings* section (pp. xii-xvi) in which a very brief history of cartography is presented. Three sections, Ab*out the Author* (pp. ix), the *Preface* (pp. x-xi), and *A (Very) Brief History of GIS* (pp. xvii-xxv) take the reader on an account of the author's unique professional life history. A detailed narrative informs us on the origins of the Environmental Systems Research Institute Inc. company, which we all know now as Esri, and Mr. Dangermond's role in the co-development of geographic information science and technology, let alone one of the most widely used software suites.

Even though the reader would have liked it, not surprisingly there is no table of contents, likely because given the depth and breadth of this work it would be extremely voluminous. A *Table of Questions* (pp. iv-v) is offered instead. Throughout its 274 pages, this book is laid out as a series of chapters, formulated as basic "What is…" geo-questions, of which there are eight: **1-** *What is the Geographic Approach* (pp. 1-37); **2-** *What is Geodata*, (pp. 38-89); 3- What is Geovisualization, (pp. 90-129); **4- What is Geommmunication**, (pp. 130-161); **5-** *What is Geoanalysis*, (pp. 162-193); **6-** *What is Geocollaboration*, (pp. 194-221); **7-** *What is Geoaccounting* and (pp. 222-237); and **8-** *What is Geodesign*. (pp. 238-261).

Geography, or the "science of where" as Esri's tagline brands it, is the author's constant assistant helping him paint the canvas anew as every new geo-question is answered not only with compelling and beautifully designed graphics, but with tangible and real-world examples of state-of-the-science-and-technology applications. The book contains connections between geography and other geospatial sciences, such as geodesy, surveying, and remote sensing for example, laying out rich expositions of their fundamental principles in conjunction with ample graphic, textual and numerical examples of their relationships with GIS and other scientific domains. Chock-full of testimonials and vignettes, this book displays throughout its pages what constitutes a veritable procession of luminaries in geography, GIS and allied disciplines. Richly illustrated, this work offers a commanding and panoramic view of topics relevant to today's challenges faced by our world, as it spares no effort in providing a plethora of visual aids, properly attributed in the *Image Credits* section (pp. 269-273). Understandably, there are virtually no pages of the book that don't show at least one figure. At a glance it seems that over half of the printed matter is covered by graphics or images, with text sometimes taking an obvious secondary role. Each geo-question deep-dives into a single case study numbered in accordance with the chapter it appears in: **Case Stude 01**: "*Integrative Wildfire Data Reporting*" (pp.33- 37); **Case Study 02**: "*Human Population, Social Justice, and Demographics*" (pp. 83-89); **Case Study 03**: "*Visualizing Geologic and Seismic Data*" (pp. 125-129); **Case Study 04**: "*Telling the Story of the Anthropocene*" (pp. 155- 161); **Case Study 05**: "*Mapping and Biodiversity*" (pp. 191-193); **Case Study 06**: "*Search and Rescue Operations*" (pp. 217-221); **Case Study 07**: "*Transit Access and Jobs in Los Angeles*" (pp. 235-237); and **Case Study 08**: "*Blending Old City Concepts with Smart City Ideals*" (pp. 259-261).

When the subject matter warrants it, the author offers detailed timelines that help the reader track the complex lineage and temporal evolution of the ideas and collaborations leading to the creation of disciplines or subdisciplines such as: *Geodata Timeline* (pp. 56-59), *Geocollaboration Timeline* (pp. 206-209) and *Geodesign Timeline* (pp. 248-251). Special interest topics are also addressed, such as *Geospatial Artificial Intelligence* (pp. 183-185), *Knowledge Graphs* (pp. 176-177) and the *United Nations Sustainable Development Goals* (SDGs) from the 2030 Agenda for Sustainable Development (pp. 230-231). It is the reader's hope that perhaps some other topics, such as *Planetary Mapping* (pp. 122-123) will be expanded in a new edition of the book. The closing sections are also insightful and also essential reading. In the Postscript section (pp. 262-263) for example, the author tells the reader that this book represents the result of half a century of collaborative effort, a life-long legacy to posterity from him and his wife Laura. A heartwarming testimonial from the team that helped the author make the book possible appears on the *How the Book Came About* section (p. 264). An army of collaborators helped bring this book to life and they are properly credited in the *Acknowledgments* section (pp. 266-268). By using a refreshing storytelling modality, this book will undoubtedly assist both professionals and laypersons alike in their efforts to further popularize the fundamentals and applications of GIS and geospatial thinking. Born with a didactic and pedagogic nature, it is our hope that this book will be used as a teaching aid in a number of activities as it connects the main subject matter to a panoply of other scientific domains. As stated on the final *See the Book Come Alive* section (p. 265), book materials can be found at https://powerofwhere.com/ which can be used to develop curriculum, module lessons, special projects and other resources throughout the educational spectrum. Even though it is never referred to as such, the "Power of Where" in essence constitutes a valuable, indispensable handbook for every geospatial professional, and as such – and until the next edition appears! it deserves to be her/his constant companion.

STAND OUT FROM THE REST

EARN ASPRS CERTIFICATION

ASPRS congratulates these recently Certified and Re-certified individuals:

RECERTIFIED PHOTOGRAMMETRIST

Jeremy Mullins, Certification # R1404CP
Effective May 26, 2024, expires May 26, 2029

Todd Andrews, Certification # R1471CP
Effective December 15, 2025, expires December 15, 2030

James Powers, Certification # R1648CP
Effective November 26, 2024, expires November 26, 2029

Byron Jordan, Certification # R1382CP
Effective December 11, 2024, expires December 11, 2029

Marvin Miller, Certification # R1025CP
Effective August 7, 2024, expires August 7, 2029

Wesley Palmer, Certification # R1638CP
Effective September 18, 2023, expires September 18, 2028

Claire Kiedrowski, Certification # R1244CP
Effective December 14, 2024, expires December 14, 2029

James Christopher Ogier, Certification # R1574CP
Effective August 21, 2024, expires August 21, 2029

Paul Montez, Certification # R1571CP
Effective August 10, 2024, expires August 10, 2029

Richard Carlson, Certification # R1232CP
Effective November 25, 2024, expires November 25, 2029

RECERTIFIED MAPPING SCIENTIST LIDAR

Thomas Prescott, Certification # R046L
Effective November 1, 2024, expires November 1, 2029

Wesley Palmer, Certification # R031L
Effective September 18, 2023, expires September 18, 2028

RECERTIFIED LIDAR TECHNOLOGIST

Andrew Ericson, Certification # R058LT
Effective December 2, 2023, expires December 2, 2026

CERTIFIED LIDAR TECHNOLOGIST

Bryan Gale, Certification # LT096
Effective November 5, 2024, expires November 5, 2027

CERTIFIED REMOTE SENSING TECHNOLOGIST

Ryan Lennon, Certification # RST245
Effective December 1, 2024, expires December 1, 2027

CERTIFIED PHOTOGRAMMETRIST

Thomas Nauke, Certification # CP1684
Effective November 9, 2024, expires November 9, 2029

ASPRS Certification validates your professional practice and experience. It differentiates you from others in the profession. For more information on the ASPRS Certification program: contact **certification@asprs.org,** visit **www.asprs.org/general/asprs-certification-program.html.**

asprs THE IMAGING & GEOSPATIAL INFORMATION SOCIETY

DR. JIE SHAN RETIRES AS HIGHLIGHT ARTICLE EDITOR FOR *PE&RS*

Jie Shan has been with ASPRS recruiting and editing highlight articles for over 15 years. During this time, he has worked with many authors in government, academia, and industry. Providing valuable insight to *PE&RS* and the geospatial community.

Dr. Shan was recently ratified as a Reilly Professor of Civil Engineering, a named professorship at Purdue University. Jie will work closely with the U.S. Geological Survey/EROS on Landsat in the next few years.

ASPRS would like to congratulate Jie on his future collaborations and thank him for his service to ASPRS and the geospatial community.

NEW ASPRS MEMBERS

ASPRS would like to welcome the following new members!

AT LARGE
Abubaker Elshikh
Andrew Esch

FLORIDA
Raison Joseph
Christopher Mulholland
Taran Polzin
Bryce Voss

GULF SOUTH
Keaton Ford
Kenneth J. Leger

HEARTLAND
A H M Mainul Islam
Melanie Lemon
Gary Paule, PLS

MID SOUTH
Meghan Touat

PACIFIC SOUTHWEST
Kaylyn Burns

POTOMAC
Dr. Sheridan Moore, Ph.D.

ROCKY MOUNTAIN
Adrian Kropp
Kelly McCoy

WESTERN GREAT LAKES
Brian Hatfield

FOR MORE INFORMATION ON ASPRS MEMBERSHIP, VISIT
HTTP://WWW.ASPRS.ORG/JOIN-NOW

The layman's perspective on technical theory and practical applications of mapping and GIS

MAPPING MATTERS

YOUR QUESTIONS ANSWERED

by Qassim Abdullah, Ph.D., PLS, CP
Woolpert Vice President and Chief Scientist

- **Have you ever wondered about what can and can't be achieved with geospatial technologies and processes?**
- **Have you been intimidated by formulas or equations in scientific journal articles and published reports?**
- **Would you like to understand the geospatial industry in layman's terms?**
- **Do you have a challenging technical question that no one you know can answer?**

If you answered "YES" to any of these questions, then you need to read Dr. Qassim Abdullah's column, Mapping Matters.

In it, he answers all geospatial questions—no matter how challenging—and offers accessible solutions.

Send your questions to Mapping_Matters@asprs.org

To browse previous articles of Mapping Matters, visit http://www.asprs.org/Mapping-Matters.html

"Your mapping matters publications have helped us a lot in refining our knowledge on the world of Photogrammetry. I always admire what you are doing to the science of Photogrammetry. Thank You Very much! the world wants more of enthusiast scientists like you."

"I read through your comments and calculations twice. It is very clear understandable. I am Honored there are experienced professionals like you, willing to help fellow members and promote knowledge in the Geo-Spatial Sciences."

YOUR COMPANION TO SUCCESS

Guest Editorial
Photogrammetric Engineering and Remote Sensing (*PE&RS*) Journal
of the American Society of Photogrammetric Engineering and Remote Sensing (ASPRS)

February 2025 Special Issue on

Hyperspectral Special Issues to Advance Remote Sensing Science

Dr. Prasad S. Thenkabail
U.S. Geological Survey (USGS)
pthenkabail@usgs.gov

Dr. Itiya Aneece
U.S. Geological Survey (USGS)
ianeece@usgs.gov

Dr. Pardhasaradhi Teluguntla
Bay Area Environmental Research Institute (BAERI) @ USGS, California, USA
pteluguntla@usgs.gov

This is the third special issue in the last 7 months on hyperspectral remote sensing in the *Photogrammetric Engineering and Remote Sensing* (*PE&RS*) journal under the special issue topic entitled "*Ushering a New Era of Hyperspectral Remote Sensing to Advance Remote Sensing Science in the Twenty-first Century*." The first was the August 2024 special issue of *PE&RS* (Thenkabail et al., 2024a), followed by the November 2024 special issue of *PE&RS* (Thenkabail et al., 2024b). Great advances are taking place in remote sensing science (Thenkabail, 2024 a,b,c,d,e,f) with a series of new generation spaceborne hyperspectral sensors, cloud computing, and artificial intelligence (Thenkabail *et al.,* 20024 a, b) being at the forefront enabling such advances.

A total of 13 hyperspectral, high spatial resolution, machine learning, deep learning, and closely related papers are published in the three *PE&RS* special issues: five in August 2024, four in November 2024, and four in the February 2025 issue (this issue). Overviews of these papers are provided for the August 2024 issue (Thenkabail *et al.*, 2024a), the November 2024 issue (Thenkabail *et al.*, 2024b), and the February 2025 issue (this introduction).

Why do we need special issues? First, hyperspectral remote sensing science is still in its nascent stages with requirements for understanding and characterization of data, exploring applications to myriad sciences, establishing clarity on where new applications and advances in existing applications can be made, and a host of other research and development areas utilizing hyperspectral data. Second, numerous new generation hyperspectral remote sensing sensors have been launched. However, the community of practice (CoP) and expertise are limited. Special issue articles will bring focus to addressing key issues pertaining to hyperspectral remote sensing science and help understand and solve them with new technologies, hence expanding the knowledge base and CoP. We encourage everyone interested in hyperspectral remote sensing science to read our two introductory editorials of the August *PE&RS* special issue (Thenkabail *et al.*, 2024a) and November *PE&RS* special issue (Thenkabail *et al.* 2024b) where we lay out the characteristics of some of the new generation hyperspectral sensors, outline the needs for hyperspectral remote sensing science research, and highlight the key goals and objectives that are critical to be addressed to advance the hyperspectral remote sensing science. Further, in those two introductory articles as well as this introductory article, and others highlighted in Thenkabail *et al.*, 2021. we provide an overview of the papers published in the three special issues.

The advent of artificial intelligence (AI) is revolutionizing all fields (Zhang and Zhang, 2022). In remote sensing, it is revolutionizing every step of remote sensing science from data collection, processing, and analysis. Many foundation models are built for geospatial AI (GAI) (Hong *et al.*, 2024, Liu *et al.*, 2024, Agapiou and Lysandrou, 2023, Mai *et al.*, 2022) including cloud-based AI on Google Earth Engine (Yang *et al.*, 2022). In this special issue, McCormick *et al.* developed an artificial neural network (ANN) multilayer perceptron (MLP) model to classify irrigated agricultural crops in a study area of California's Central Valley (CCV). The ANN MLP model is trained using the United States Department of Agriculture's (USDA) Cropland Data Layer (CDL) reference data on crop types. The goal of the ANN MLP model is to train itself using the USDA CDL reference data as knowledge on crop types utilizing Harmonized Landsat-8 Sentinel-2 (HLS) Landsat 30m (L30) data (HLSL30). The advantage of using HLSL30 alongside HLSS30 is its global coverage every 2-3 days (from two satellites: Landsat 8 and Landsat 9 and the Sentinel-2A and 2B) in 11 spectral bands that includes visible and near infrared (VNIR) and thermal infrared (TIR) bands. Once the ANN MLP is well-trained for identifying crops, it is applied to Landsat data for independent years to automatically use its trained intelligence to identify crop types. The paper by McCormick *et al.* developed the crop type identification ANN MLP model based on year 2021 HLSL30 data and applied it to identify crop types using its developed intelligence to identify crop types for independent year 2022 using HLSL30 data and achieving high overall, producer's and user's accuracies.

The paper on monitoring forest fires with MODIS time-series by Azimuddin and Dwivedi is timely. With the recent devastating fires of California of January 2025, the need for appropriate remote sensing data to monitor active fires for swift action as well as post-fire assessment of damage is critical. Although Azimuddin and Dwivedi did not use hyperspectral data, their study on detecting and reporting fires in Uttarakhand, India is universally relevant. They use MODIS C6 active fire point products to study fires in Uttarakhand over 15 years. Their study highlights the usefulness as well as limitations of coarse-resolution MODIS data in detecting fires. Fire studies require remote sensing images acquired at very high spatial, spectral, temporal, and radiometric resolution: either near-continuous observations over fire-prone areas or at least every 10-15 minutes as the authors point out. Thermal data to study fires is also a must to gather the temperature intensity of fires. However, one of the least explored remote sensing data in fire studies is hyperspectral data. The hyperspectral signature banks of fires of various intensities as well as spectral signature banks of fires before, during, and after fire are of great importance to advance fire science. It must be noted that the time-series remote sensing data such as the HLSL30 will have hundreds or thousands of bands of data stacked as analysis-ready data-cubes (ARDs) when seasonal, yearly, or multi-year data streams are used for analysis. This is akin to hyperspectral data-cubes with hundreds and thousands of bands of data. This is where the hyperspectral and multispectral data analysis techniques, methods, and approaches can have a lot in common.

The paper by Ma *et al.*, develops advanced deep learning and climbing methods and techniques for individual tree segmentation in complex forest structures using unmanned aircraft system (UAS) point cloud airborne lidar scanning (ALS) data. The authors establish impressive accuracies. However, such studies lack spectral profiles of trees that will help identify tree types, tree species, and their biophysical and biochemical characteristics. Forest studies are ideally advanced by a combination of remote sensing data such as hyperspectral and LiDAR data.

Further, the paper by Sun *et al.* explores the methods and techniques for detecting ships (small and big) accurately using multi-sensor remote sensing data. As expected, high spatial resolution imagery is the best to detect small ships in particular. However, analysis requires Feature Enhancements in the images, utilization of other ancillary data in the image to detect the ships, and smart algorithms like Multi-scale Perception that the authors propose. Yet, these methods and techniques can be very tedious and computationally intensive. Uncertainties in ship detection are still significant. Hyperspectral data when acquired in sufficient high spatial resolution (e.g., 1-5 m) and in sufficient temporal frequency (e.g., every few minutes) should help acquire very high levels of accuracy in ship detection.

Finally, we want to highlight the latest new generation spaceborne imaging spectroscopy data from German Space Agency's EnMAP (Environmental Mapping and Analysis Program) imaging spectroscopy in characterizing agricultural crops (Figure 1). We illustrate this in Figure 1 taking almond and grape crops in California's Central Valley. The hyperspectral signatures derived from EnMAP tell many subtle stories that will help classify crops and quantify them to study many plant quantitative parameters such as their biophysical properties (e.g., biomass, leaf area index, plant height), biochemical properties (e.g., nitrogen, lignin, chlorophyll, pigments like carotenoids and anthocyanins), plant moisture and water, plant health and stress, and plant structural properties (e.g, planophile, eroctophile). These parameters of plants can be studied using full spectrum and\or specific bands for specific quantities (e.g., 970 nm for water absorption or 680 nm for chlorophyll; Figure 1).

Acknowledgements

Any use of trade, firm, or product names is for descriptive purposes only and does not imply endorsement by the U.S. Government.

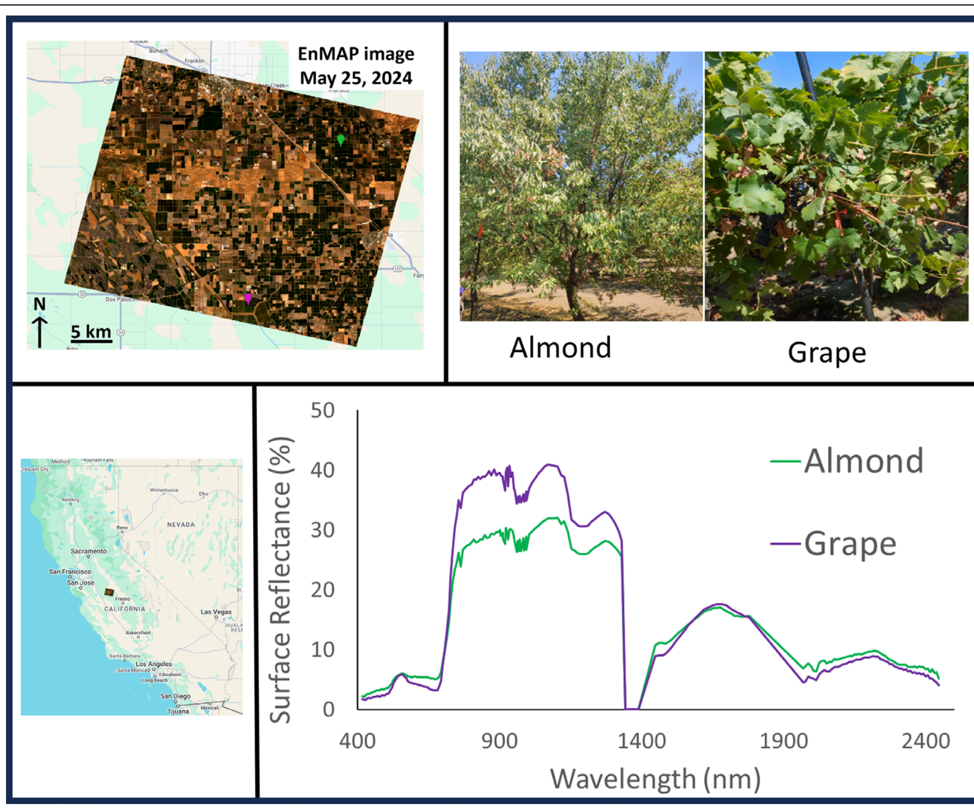

Figure 1. EnMAP imaging spectroscopy data to characterize agricultural crops. Figure shows hyperspectral signatures of two crops: Almonds and Grapes derived from German Space Agency's EnMAP (Environmental Mapping and Analysis Program) data acquired on May 25, 2024, over a study area in California's Central Valley. The EnMAP data are depicted in RGB hyperspectral narrowband (HNB) centers @662 nm, 530 nm, and 450 nm [each band with 10 nm bandwidth]. EnMAP acquires data in 244 HNBs over the 420-2440 nm spectral range and in 10 nm bandwidths. The hyperspectral signatures show grape with high absorption in the red band ranges (600-700 nm) and high reflectivity in near infrared (NIR) (740-900 nm). In contrast the Almond has significantly higher reflectivity in the red and and lower reflectivity in NIR. This is because of less background soil reflectivity in grapes having higher canopy cover in 30m pixel of EnMAP as well as greater vigor and nitrogen content of the grape plant. Also observe plant water absorption in 960 nm and 1240 nm. These bands depict plant water content. Indeed, the entire spectral signature as well as specific portions of the hyperspectral narrowbands have a story to tell about the biophysical, biochemical, plant health, plant stress, and plant structural properties.

References

Agapiou, A.; Lysandrou, V. 2023. Interacting with the Artificial Intelligence (AI) Language Model ChatGPT: A Synopsis of Earth Observation and Remote Sensing in Archaeology. *Heritage* 2023, 6, 4072-4085. https://doi.org/10.3390/heritage6050214

Hong *et al.*, 2024. "SpectralGPT: Spectral Remote Sensing Foundation Model," in *IEEE Transactions on Pattern Analysis and Machine Intelligence*, vol. 46, no. 8, pp. 5227-5244, Aug. 2024, doi: 10.1109/TPAMI.2024.3362475

Liu *et al.*, 2024. "RemoteCLIP: A Vision Language Foundation Model for Remote Sensing," in *IEEE Transactions on Geoscience and Remote Sensing*, vol. 62, pp. 1-16, 2024, Art no. 5622216, doi: 10.1109/TGRS.2024.3390838.

Mai, G., Cundy, C., Choi, K., Hu, Y., Lao, N., and Ermon. S. 2022. Towards a foundation model for geospatial artificial intelligence (vision paper). In *Proceedings of the 30th International Conference on Advances in Geographic Information Systems* (SIGSPATIAL '22). Association for Computing Machinery, New York, NY, USA, Article 106, 1–4. https://doi.org/10.1145/3557915.3561043

Thenkabail, P.S., Aneece, I., Teluguntla, P. 2024a. Special Issue Introduction: Ushering a New Era of Hyperspectral Remote Sensing to Advance Remote Sensing Science in the Twenty-first Century. *PE&RS* Special Issue. *Photogrammetric Engineering and Remote Sensing*. 90(8): 467-470. Doi: 10.14358.PERS.90.8.467. https://www.ingentaconnect.com/contentone/asprs/pers/2024/00000090/00000008/art00006

Thenkabail, P.S., Aneece, I., and Teluguntla (Editorial). 2024b. New Generation Hyperspectral Data for Quantum Leap in Remote Sensing Science for Agriculture. *Photogrammetric Engineering & Remote Sensing*. Vol. 90, No. 11, November 2024, pp. 661–663. 0099-1112/22/661–663. doi: 10.14358/PERS.661-663. https://www.ingentaconnect.com/contentone/asprs/pers/2024/00000090/00000011/art00008

Thenkabail, Prasad. 2024a. *Remote Sensing Handbook (Second Edition, Six Volume Book-set), Volume I: Sensors, Data Normalization, Harmonization, Cloud Computing, and Accuracies.* Taylor and Francis Inc.\CRC Press, Boca Raton, London, New York. 978-1-032-89095-1— CAT# T132478. Print ISBN: 9781032890951. eBook ISBN: 9781003541141. Pp. 640.

Thenkabail, Prasad. 2024b. *Remote Sensing Handbook (Second Edition, Six Volume Book-set), Volume II: Image Processing*, Change Detection, GIS, and Spatial Data Analysis. Taylor and Francis Inc.\CRC Press, Boca Raton, London, New York. 978-1-032-89097-5— CAT# T133208. Print ISBN: 9781032890975. eBook ISBN: 9781003541158. Pp. 552.

Thenkabail, Prasad. 2024c. *Remote Sensing Handbook (Second Edition, Six Volume Book-set), Volume III: Agriculture, Food Security, Rangelands, Vegetation, Phenology, and Soils*. Taylor and Francis Inc.\CRC Press, Boca Raton, London, New York. 978-1-032-89101-9 —CAT# T133213. Print ISBN: 9781032891019; eBook ISBN: 9781003541165. Pp. 824.

Thenkabail, Prasad. 2024d. Remote Sensing Handbook (Second Edition, Six Volume Book-set), Volume IV: Forests, Biodiversity, Ecology, LULC, and Carbon. Taylor and Francis Inc.\CRC Press, Boca Raton, London, New York. 978-1-032-89103-3— CAT# T133215. Print ISBN: 9781032891033. eBook ISBN: 9781003541172. Pp. 568.

Thenkabail, Prasad. 2024e. *Remote Sensing Handbook (Second Edition, Six Volume Book-set), Volume V: Water, Hydrology, Floods, Snow and Ice, Wetlands, and Water Productivity*. Taylor and Francis Inc.\CRC Press, Boca Raton, London, New York. 978-1-032-89145-3 — CAT# T133261. Print ISBN: 9781032891453. eBook ISBN: 9781003541400. Pp. 592.

Thenkabail, Prasad. 2024f. Remote Sensing Handbook (Second Edition, Six Volume Book-set), Volume VI: Droughts, Disasters, Pollution, and Urban Mapping. Taylor and Francis Inc.\CRC Press, Boca Raton, London, New York. 978-1-032-89148-4 — CAT# T133267. Print ISBN: 9781032891484; eBook ISBN: 9781003541417. Pp. 520.

Thenkabail, P.S., Aneece, I., Teluguntla, P., Oliphant, A. 2021. Hyperspectral Narrowband Data Propel Gigantic Leap in the Earth Remote Sensing. Highlight Article. *Photogrammetric Engineering and Remote Sensing*. http://www.asprs.org/a/publications/pers/2021journals/07-21_July_Flipping_Public.pdf doi: 10.14358/PERS.87.7.461. 87(7): 461-467. IP-127022.

Zhang and Zhang, 2022. "Artificial Intelligence for Remote Sensing Data Analysis: A review of challenges and opportunities," in *IEEE Geoscience and Remote Sensing Magazine*, vol. 10, no. 2, pp. 270-294, June 2022, doi: 10.1109/MGRS.2022.3145854.

Spatiotemporal Behavior of Active Forest Fires Using Time-Series MODIS C6 Data

Syed Azimuddin and R.S. Dwivedi

Abstract

Forest fires have a profound influence on the economy, ecology, and environment. Realizing the potential of remote sensing in forest fire management, a study was taken up to investigate the spatiotemporal behavior of active forest fires in a mountainous terrain of Uttarakhand State, north India, using 15 years' time-series historical MODIS (C6) active fire point products. Results indicate an overall fire incidence detection accuracy of 62.3% with a KHAT value of 0.59. Moreover, a regular trend in intra-annual behavior in fire incidences with peaks during the hot and dry period of the year was observed and a large year-to-year variability in fire regimes with no significant trends over time could be noticed. The approach and results are discussed in detail along with the future perspective.

Introduction

Forest fires play a pivotal role in modulating ecological processes and ecosystem services in terms of changes in terrestrial carbon stocks; structure and spatial distribution of vegetation; and variations in water and energy fluxes, apart from influencing human health and socioeconomic conditions. Real-time information on incidents of active fires and their drivers is a prerequisite for planning strategies and formulating policies for their management. Traditionally, fire towers in forested areas have been used for detection of forest fires; these do not meet the requirements of forest fire management, apart from being unreliable and time and cost prohibitive.

Spaceborne remote sensing data have been used globally for over four and a half decades for biomass burning–related fires (Hitchcock and Hoffer 1974; Dozier 1981; Wolfe *et al.* 1998; Lentile *et al.* 2006; Giglio *et al.* 2009; Kumar and Roy 2018; Briones-Herrera *et al.* 2020). Forest fires exhibit higher emittance in the middle and thermal regions of electromagnetic radiation as compared with other terrestrial features (López García and Caselles 1991). Thermal infrared (TIR) channel data (3.6–12 μm) from coarse-spatial-resolution orbital sensors such as the Advanced Very High Resolution Radiometer (Cahoon *et al.* 1994), the Along Track Scanning Radiometer, or the Moderate Resolution Imaging Spectroradiometer (MODIS) have been used for detection of active forest fires. Moreover, higher thermal contrast of active fires in comparison with the surrounding background permits reliable detection of active fires of even as small as less than 0.01% of a 1-km² pixel (Robinson 1991).

The launch of the *Terra* satellite in 1999 with MODIS capable of imaging the Earth in the near-infrared, short-wave infrared, and TIR channels with a repeat cycle of 16 days heralded a new era in detection of active forest fires and wildfires (Wolfe *et al.* 1998). The launch of the *Aqua* satellite with MODIS aboard, with the same payload as that of *Terra*, in 2002, further augmented this capability. In fact, the twin sensors, the *Aqua* MODIS and the *Terra* MODIS, acquire data twice daily, i.e., at 1:30 PM and 1:30 AM and at 10:30 AM and 10:30 PM, respectively, providing four near-global coverages daily (Wolfe *et al.* 2002). With a 110° field of view, a MODIS swath covers a width of 2340 km (Wolfe *et al.* 2002) with spatial resolutions of 250 m, 500 m, and 1 km in visible-near-infrared, short-wave infrared, and TIR, respectively, which are very useful for regional-level detection of active forest fires.

Syed Azimuddin is with Cognizant Technology Solutions India Pvt. Ltd., DLF Building Block-1, Plot#129-132, APHB Colony Gachibowli, Hyderabad 500 019, India (sdazeem106@gmail.com).

R.S. Dwivedi is with Jawaharlal Nehru Technological University, Hyderabad, Telangana-500085, India.

Corresponding author: Ravi Dwivedi (rsdwivedi51@gmail.com)

Received March 14, 2024, accepted April 13, 2024.

Material and Methods

Test Site

Covering a geographical area of 53 483 km², Uttarakhand State, the study area, is bordered to the northwest by Himachal Pradesh, to the northeast by Tibet, to the southeast by Nepal, and to the south and southwest by Uttar Pradesh (Figure 1). Most of the terrain of Uttarakhand is mountainous. Physiographically, the state consists of (1) the northern zone, commonly known as the Himadri (snow-covered area), with elevations ranging roughly from 3000 to 7600 m; (2) the Lesser Himalayas, with elevations ranging between about 2000 to 3000 m; (3) the Siwalik range; (4) a narrow bed of gravel and alluvium known as the Bhabar (piedmont zone), which interfaces to the southeast with the marshy terrain known as the Tarai (marshy land); and (5) flat-floored depressions in the south of the Siwaliks known locally as *duns*. The elevation in the Siwalik-Bhabar-Tarai area ranges from 300 to 3000 m.

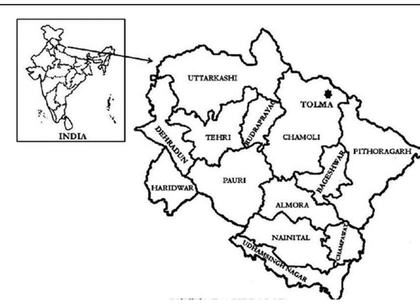

Figure 1. Location map of the test site.

The climate of Uttarakhand is highly variable. It varies from subtropical at the lower elevation to alpine at higher elevations above timberline. The area experiences a mean summer temperature of 30°C and a mean winter temperature of 18°C. The hilly regions receive precipitation in the range of 600 to 1000 mm. Of this, around 30% is received as snow during the winter and the balance is received as rain during the middle of June to September. May and June experience very high temperatures that are accompanied by low humidity. This period coincides with incidences of forest fire expansion. Overcast conditions in Uttarakhand State range from 1 day in November to 13 days in July, with an annual cloud cover of 66 days at 5:30 PM and 62 days at 7:30

Photogrammetric Engineering & Remote Sensing
Vol. 91, No. 2, February 2025, pp. 85–90.
0099-1112/22/85–90

doi: 10.14358/PERS.24-00035R2

PEER-REVIEWED CONTENT
IS ONLY AVAILABLE TO
ASPRS MEMBERS AND SUBSCRIBERS

FOR MORE INFORMATION VISIT
MY.ASPRS.ORG

PEER-REVIEWED CONTENT IS ONLY AVAILABLE TO ASPRS MEMBERS AND SUBSCRIBERS

FOR MORE INFORMATION VISIT MY.ASPRS.ORG

PEER-REVIEWED CONTENT
IS ONLY AVAILABLE TO
ASPRS MEMBERS AND SUBSCRIBERS

FOR MORE INFORMATION VISIT
MY.ASPRS.ORG

**PEER-REVIEWED CONTENT
IS ONLY AVAILABLE TO
ASPRS MEMBERS AND SUBSCRIBERS**

**FOR MORE INFORMATION VISIT
MY.ASPRS.ORG**

PEER-REVIEWED CONTENT IS ONLY AVAILABLE TO ASPRS MEMBERS AND SUBSCRIBERS

FOR MORE INFORMATION VISIT MY.ASPRS.ORG

In-Press

Accuracy Assessment of Dense Point Cloud Generated by Deep Learning and Semiglobal Matching
Haval AbdulJabbar Sadeq

A Comparative Study of Deep Learning Methods for Automated Road Network Extraction from High-Spatial-Resolution Remotely Sensed Imagery
Haochen Zhou, Hongjie He, Linlin Xu, Lingfe Ma, Dedong Zhang, Nan Chen, Michael A. Chapman, and Jonathan Li

Real-time Vanishing Point Tracking in Manhattan World Using Improved BaySAC
Chenming Ye, Zhizhong Kang, Jinhao Cai, and Longze Zhu

SAT2BUILDING: LoD-2 Building Reconstruction from Satellite Imagery Using Spatial Embeddings
Philipp Schuegraf, Shengxi Gui, Rongjun Qin, Friedrich Fraundorfer, and Ksenia Bittner

The Aboveground Carbon Stock of Moso Bamboo Forests Is Significantly Reduced by *Pantana phyllostachysae* Chao Stress: Evidence from Multi-source Remote Sensing Imagery
Yuanyao Yang, Zhanghua Xu, Lingyan Chen, Wanling Shen, Haitao Li, Chaofei Zhang, Lei Sun, Xiaoyu Guo, and Fengying Guan

Cost-Effective High-Definition Building Mapping: Box-Supervised Rooftop Delineation Using High-Resolution Remote Sensing Imagery
Hongjie He

Artificial Neural Network Multi-layer Perceptron Models to Classify California's Crops using Harmonized Landsat Sentinel (HLS) Data

Richard McCormick, Prasad S. Thenkabail, Itiya Aneece, Pardhasaradhi Teluguntla, Adam J. Oliphant, and Daniel Foley

Abstract

Advances in remote sensing and machine learning are enhancing cropland classification, vital for global food and water security. We used multispectral Harmonized Landsat 8 Sentinel-2 (HLS) 30-m data in an artificial neural network (ANN) multi-layer perceptron (MLP) model to classify five crop classes (cotton, alfalfa, tree crops, grapes, and others) in California's Central Valley. The ANN MLP model, trained on 2021 data from the United States Department of Agriculture's Cropland Data Layer, was validated by classifying crops for an independent year, 2022. Across the five crop classes, the overall accuracy was 74%. Producer's and user's accuracies ranged from 65% to 87%, with cotton achieving the highest accuracies. The study highlights the potential of using deep learning with HLS time series data for accurate global crop classification.

Introduction

Agricultural research is critical to managing and maintaining finite food and water resources around the world. The ability to accurately map croplands is essential to prospective scientific endeavors such as mapping and monitoring global crop water productivity (Foley *et al.* 2023), ensuring global food security (Gumma *et al.* 2022), and promoting general welfare through informed policymaking (Bégué *et al.* 2020). Remote sensing has played a long and important role in expanding the opportunities available in the scientific exploration of agriculture (Ozdogan *et al.* 2010; Karthikeyan *et al.* 2020; Khanal *et al.* 2020; Martos *et al.* 2021), such as regional and global cropland classification products to support food and water security (Thenkabail, Teluguntla, *et al.* 2021; Valero *et al.* 2016; Xiong *et al.* 2017; Teluguntla *et al.* 2018, 2023; Parreiras *et al.* 2022). Expanding these efforts offers unprecedented new opportunities to classify and map croplands throughout the world in the service of global resource security.

Although hyperspectral data have been successfully used for crop type classification and have shown significant advances in mapping, modeling, and monitoring various crop characteristics (Thenkabail, Aneece, *et al.* 2021; Aneece and Thenkabail 2022; Khan *et al.* 2022; Yu *et al.* 2022), they are acquired only through tasking, limiting their availability (Lu *et al.* 2019). On the other hand, multispectral platforms collect data regularly (Miller *et al.* 2019). The Landsat series of sensors provides a substantial archive of imagery time series since 1972 throughout the world (Wulder *et al.* 2022). Sentinel-2A and Sentinel-2B, designed to be compatible with the Landsat sensors, further contribute to data availability (Falanga Bolognesi *et al.* 2020). The recently available Harmonized Landsat 8 Sentinel-2 (HLS) product was made to remove discrepancies across the US Geological Survey's (USGS's) and National Aeronautics and Space Administration's Landsat 8 sensor and the European Space Agency's Sentinel-2 sensor due to slight differences in spatial alignments, spectral band ranges, and view geometries (Claverie *et al.* 2018; Masek *et al.* 2018, 2021; Falanga Bolognesi *et al.* 2020; Parreiras *et al.* 2022). Harmonization was done so the two datasets could be combined more easily for analyses (Falanga Bolognesi *et al.* 2020; Parreiras *et al.* 2022). With data from both sensors combined, the HLSL30 (HLS Landsat 8 data at 30 m) and HLSS30 (HLS Sentinel-2 data at 30 m) products provide a global 30-m product with revisit times of one to four days (Falanga Bolognesi *et al.* 2020; Hong *et al.* 2023; Parreiras *et al.* 2022). HLS has provided breakthroughs in time series remote sensing analyses for various applications, including land cover classification (Falanga Bolognesi *et al.* 2020), crop classification (Parreiras *et al.* 2022; Teke 2022; Chen *et al.* 2024), estimation of crop green-up and emergence dates (Gao *et al.* 2021), cropping intensity classification (Hu *et al.* 2023), and detection of cropland abandonment (Hong *et al.* 2023). In this study, we used the HLSL30 product, which is now available in the Google Earth Engine (GEE; Gorelick *et al.* 2017) data catalog.

Within the realm of remote sensing, many machine learning (ML) algorithms have been used to classify croplands, including random forest (RF) (Xiong *et al.* 2017; Teluguntla *et al.* 2018; Oliphant *et al.* 2019) and support vector machines (SVM) (Xiong *et al.* 2017; Kang *et al.* 2018; Aneece and Thenkabail 2022). These ML algorithms, although useful and productive in their own right, suffer from the need for extensive and accurate reference training, testing, and validation data, which are resource intensive and costly to acquire; high computational cost during training; and difficulty in selecting for optimal parameters (Cervantes *et al.* 2020), and can struggle to perform when data suffer from the effects of time-specific external factors such as seasonal patterns of precipitation, temperature, etc. (Zhu 2020). Deep learning (DL) models can outperform these ML algorithms (Teke 2022). Although not entirely free of similar shortcomings to ML models, DL models are able to predict classifications faster than other models once they are trained, and have been successfully used to classify land use via remote sensing data (Cai *et al.* 2018). Multi-layer perceptron (MLP) models are a type of artificial neural network (ANN) DL model (Maleki *et al.* 2023) usually consisting of an input layer, one or more hidden layers, and an output layer (Karasu and Altan 2022; Ahmed 2023), although deep MLP models also exist (Tripathi *et al.* 2022). MLPs have been used for several applications, including gap filling for missing data (Moon *et al.* 2019) and classification of land use and land use change over time (Costa *et al.* 2015; Shen *et al.* 2020). Specific agricultural applications include crop yield prediction (Nosratabadi *et al.* 2021; Bazrafshan *et al.* 2022; Tripathi *et al.* 2022;

Richard McCormick, Prasad S. Thenkabail, Itiya Aneece, Adam J. Oliphant, and Daniel Foley are with the US Geological Survey, Western Geographic Science Center, Flagstaff AZ 86001 (rmccormick@usgs.gov, pthenkabail@usgs.gov, ianeece@usgs.gov, aoliphant@usgs.gov, dfoley@usgs.gov).

Pardhasaradhi Teluguntla is with the Bay Area Environmental Research Institute, and the US Geological Survey, Western Geographic Science Center, Flagstaff AZ 86001 (pteluguntla@usgs.gov).

Corresponding author: Itiya Aneece (ianeece@usgs.gov)

Received June 7, 2024, accepted September 20, 2024.

Photogrammetric Engineering & Remote Sensing
Vol. 91, No. 2, February 2025, pp. 91–100.
0099-1112/22/91–100

doi: 10.14358/PERS.24-00072R3

Ahmed 2023), weed detection (Karasu and Altan 2022), crop residue cover detection (Wang *et al.* 2023), crop type classification (He and Chen 2021; Wu *et al.* 2022; Maleki *et al.* 2023), and crop genotype classification (Inocente *et al.* 2022). MLP models have outperformed traditional ML models such as SVM and RF (He and Chen 2021; Wu *et al.* 2022; Yang *et al.* 2023) and other, more complex, DL models (He and Chen 2021; Wu *et al.* 2022).

Given the above, the overarching goal of this paper was to classify and map five agricultural crop classes (cotton, alfalfa, tree crops, grapes, and other) in a study area located within California's Central Valley (CCV) near Fresno, California, United States, using an ANN MLP model and HLSL30 data. These crop classes are dominant throughout the globe (and hence called world crops), and/or have high water demands that are directly influenced by national and regional policies (Foley *et al.* 2023). Thus, it is crucial to develop the capacity to map these crops using remote sensing platforms reliably and accurately. Specific objectives for this study were to:

1. Develop and implement an ANN MLP model to classify five irrigated crops in CCV;
2. Implement the model on an independent year;
3. Assess accuracies, errors, and uncertainties of the model in classifying crops using HLSL30 data.

Data and Methods

Study Area

We conducted this research in a 553.86-km² study area near Fresno, California (Figure 1). The area was selected because of high prevalence of water-intensive crops, and because it was representative of CCV (Foley *et al.* 2023). The CCV is a north-south-trending elongated valley bordered by the Coast Range to the west and the Sierra Nevada to the east. Our study area lies in the southern half of the CCV within the San Joaquin basin (Figure 1). The area contains a large diversity of row, paddy, orchard, and vineyard crops, making it ideal for assessing the growth of various crops over multiple years. The study area has higher than US average sunshine hours per year (Visher, 1954), predictably warm temperatures (DelSole *et al.* 2017), and lower than

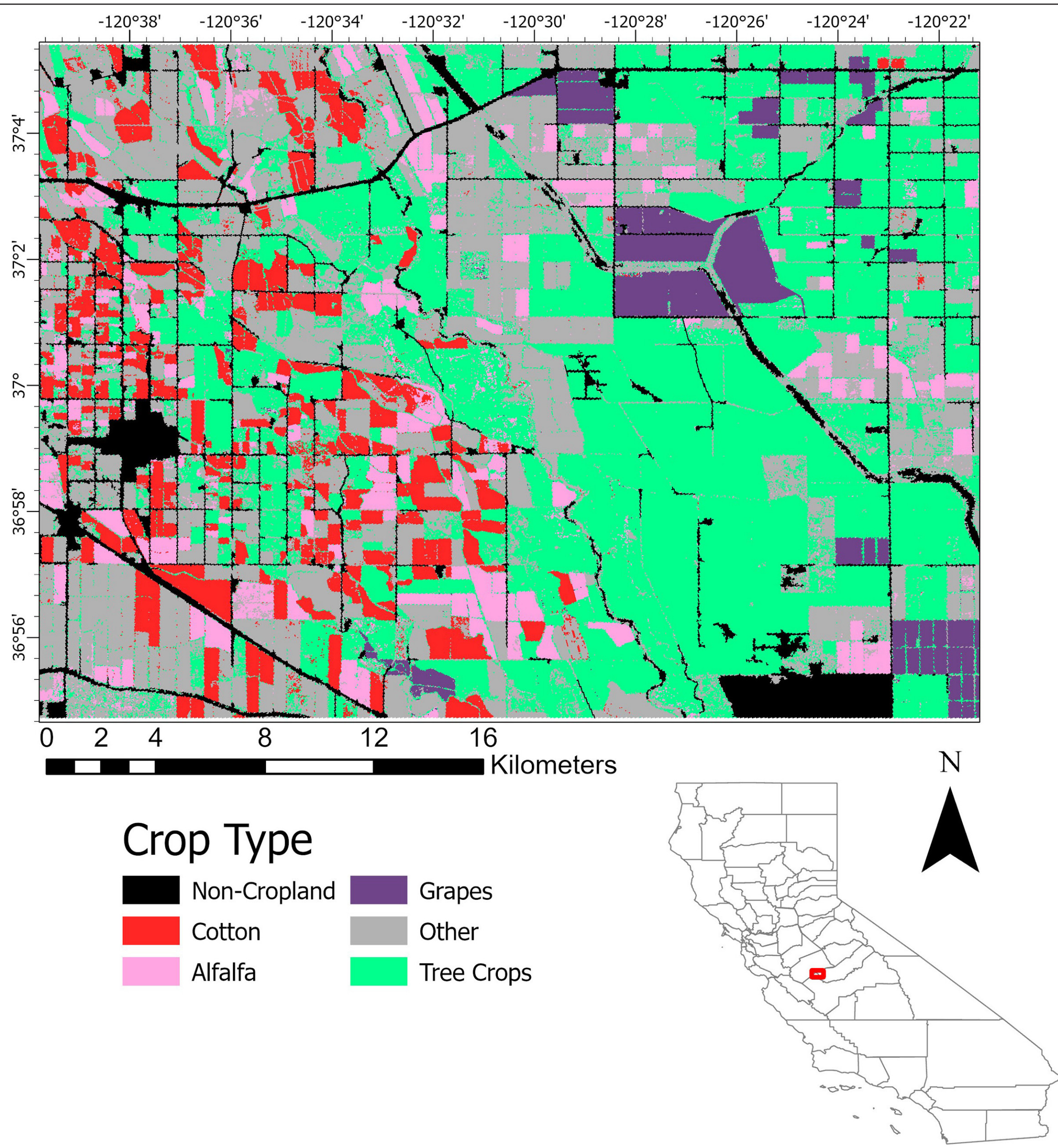

Figure 1. Study area near Fresno, California, United States. Crop type data from the US Department of Agriculture (USDA) National Agricultural Statistics Service (NASS) Cropland Data Layer (CDL) 2021 (USDA NASS 2022b).

average precipitation days (Bartels *et al.* 2020). These conditions are ideal for creating annual composites of satellite imagery, as there is reduced cloud cover and minimal overcast throughout the year.

Reference Data

The Cropland Data Layer (CDL) is provided by the US Department of Agriculture (USDA) National Agricultural Statistics Service (NASS) (USDA NASS 2022b). The dataset, produced every year since 1997 for parts of the US and since 2008 for all of the conterminous US (CONUS), maps crop types using remote sensing data and the USDA's Farm Services Agency Common Land Unit data (Teke 2022). The USDA CDL was selected for use as reference data because of high classification accuracies for the study crops (Table 1), wall-to-wall coverage of CONUS, and use by many other researchers (Konduri *et al.* 2020; Li, Chen, *et al.* 2020; Li, Zhang, *et al.* 2020; Zhang *et al.* 2022). Table 1 shows the crop distribution within the study area as represented by the CDL for the year 2021, and crop-specific classification accuracies for the same year.

For the purposes of our study, pistachios and almonds were combined into a single tree crop class. Within the study area, the only pistachio tree plantations were relatively young (five years old or less). It was observed during ground validation that the majority of the ground area within pistachio fields was bare earth (Figure 2), with the young trees not grown enough to comprise a large portion of a pixel footprint. This resulted in the spectral profiles of these crops being highly affected by bare ground. This necessitated the combination of tree crops into a single category for classification.

Table 1. Crop cover by type within study area ordered by dominance, US Department of Agriculture National Agricultural Statistics Service Cropland Data Layer for California, 2021. [Source: USDA NASS 2022a]

Crop	Area (%)	Producer's Accuracy (%)	User's Accuracy (%)
Almonds	35	90.1	87.5
Pistachios	11	89.1	89.7
Cotton	11	85.6	84.9
Alfalfa	10	86.5	81.7
Grapes	5	82.5	74.2
Other Crops	28	—	—

Remote Sensing Data

Time series imagery facilitates crop mapping by capturing different phenological stages throughout the year and the growing season (Yang *et al.* 2023). HLSL30 surface reflectance data for the study area were accessed and processed through GEE. The HLSL30 product provides 30-m nadir bidirectional reflectance distribution function–adjusted reflectance and is derived from Landsat 8/9 Operational Land Imager (OLI) data products (Masek *et al.* 2021). The HLSS30 and HLSL30 products are gridded to the same resolution and Military Grid Reference System tiling system, and thus are stackable for time series analysis (Masek *et al.* 2021).

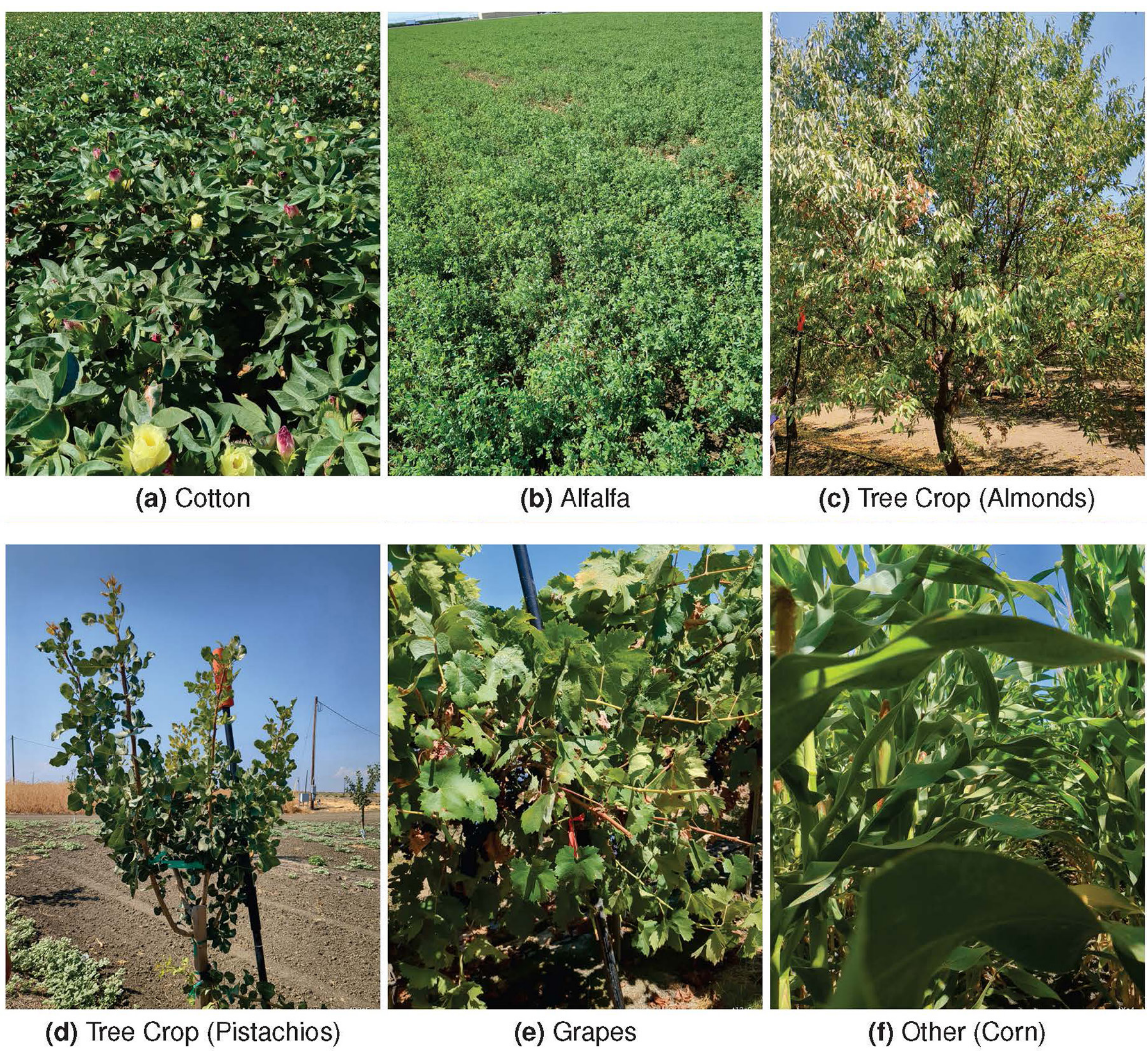

Figure 2. Crop classes. Crop fields from the study area: (a) cotton, (b) alfalfa, (c) tree crop (almonds), (d) tree crop (pistachios), (e) grapes, and (f) other (corn). [Photo credit: Adam Oliphant]

Training data for the model were selected for January–December 2021 with crop type labels provided from the USDA CDL 2021 reference training data. All cloud-free pixels were sampled to build the training dataset. A randomly selected 10% of training data was withheld for model validation. The reference testing data were selected for January–December 2022 using USDA CDL 2022 labels. As with the training data, all cloud-free pixels were sampled to build the testing dataset. The annual period (January–December 2021 for training; January–December 2022 for testing) were appended with a preceding month (December) at the beginning of the annual time series and with a subsequent month (January) at the end of the annual time series to ensure the entire cropping calendar was fully captured in the temporal linear interpolation process (detailed in "Data Preprocessing" below). Six HLSL30 bands were selected: blue, green, red, near-infrared (NIR) narrow, shortwave infrared 1, and shortwave infrared 2 (Table 2). All spectral bands have a 30 m spatial resolution, with a temporal resolution of two to three days.

Table 2. Harmonized Landsat Sentinel-2 L-30 (HLSL30) spectral bands used for this study and their wavelengths.

Band	Name	Wavelength (μm)
2	Blue	0.45–0.51
3	Green	0.53–0.59
4	Red	0.64–0.67
5	NIR	0.85–0.88
6	SWIR1	1.57–1.65
7	SWIR2	2.11–2.29

NIR = near-infrared; SWIR1 = shortwave infrared 1; SWIR2 = shortwave infrared 2.

Data Preprocessing

Extensive preprocessing was performed on the data to increase image clarity and classification performance. Overall, every month, there were approximately 10 HLSL30 images, leading to an average of 60 bands of data (6 bands × 10 images). Each band was processed for surface reflectance (%) maximum value composite (MVC), reducing the 10 bands (1 band × 10 images per month) to a single MVC surface reflectance band. The process was repeated for each of the six bands, leading to six MVC surface reflectance bands for a total of 72 surface reflectance MVC bands in a calendar year (6 MVC bands × 12 months). Monthly median Normalized Difference Vegetation Index (NDVI) bands added another 12 bands. Further, NDVI was summed across every three months for an additional four seasonal NDVI bands. Finally, one cumulative NDVI band was generated for an entire year, leading to an overall total of 89 bands (72 + 12 + 4 + 1) over one calendar year (Figure 3). The preprocessing steps are further described below.

HLSL30 Imagery Acquisition and Filtering

Within GEE, the HLSL30 data were imported and filtered to the bounds of the study area and years of interest. To facilitate temporal-gap filling, a nominal year of interest was considered to be 14 months, from December of the previous year to January of the following year.

Cloud and Cloud-Aerosol Masking

Using the Cloud Probability bitmask of HLSL30, clouds (bit 1) and cloud shadows (bit 3) were selected and removed from each image in the image collection. The resulting image collection contained images with all clouds and cloud shadows masked out, leaving only clear images remaining. When images were composited, this step ensured that composites contained only unobscured ground-level imagery, and would not be distorted or otherwise affected by cloud cover.

Masking Out Noncropland Areas

Using the Landsat-derived global rainfed and irrigated-cropland product (Thenkabail, Teluguntla, *et al.* 2021; Teluguntla *et al.* 2023), noncropland areas were masked from the image collection. This ensured only croplands were trained on and classified in the model. As the model is only to classify croplands into specific categories, there is no need to include areas that do not contain croplands.

Compositing the Images into Monthly Composites

The masked image collection was composited into a collection of 12 images, with one image for each month of the year of interest. For each month, the image collection so far was filtered to contain only images from that month. For each band in the image, each pixel in the area of interest was filled with the median value from the filtered collection. This process was repeated for each month in the year. The resulting image collection contained 12 images, each with the clearest possible band values for their respective months.

Calculating and Adding NDVI Bands

In addition to the six HLSL30 bands, the NDVI was used as a spectral indicator of plant greenness (Tucker 1979). NDVI was calculated for each month, season, and year, and added as new bands for each image collection. It was calculated from the HLSL30 data using NIR and red (RED) bands, and added as a separate band for each month (Equation 1). The median NDVI value was calculated when multiple cloud-free images were available for one month. For every three months (one

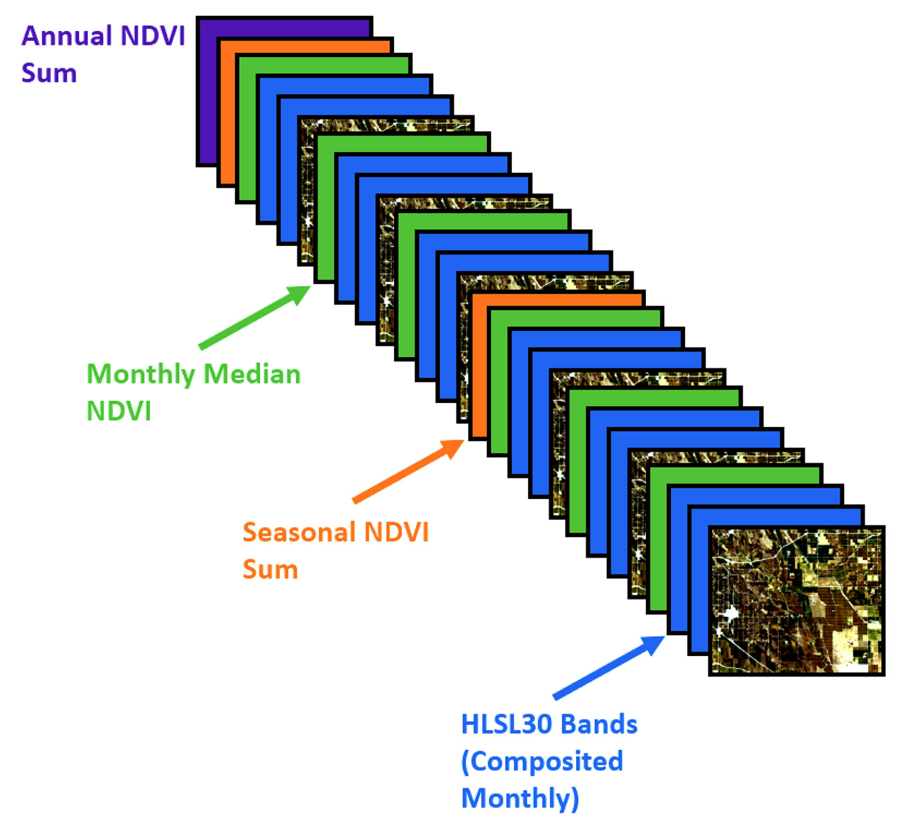

Figure 3. Illustration of Harmonized Landsat Sentinel-2 L30 (HLSL30) 1-year data cube after processing. The 89-band data cube consisted of 72 median value composite (MVC) bands (6 bands per month × 12 months); 12 monthly median Normalized Difference Vegetation Index (NDVI) bands; four cumulative seasonal NDVI bands; and one cumulative annual NDVI band.

season), NDVI was summed into a separate band (Equation 2). An annual NDVI sum band was also calculated (Equation 3).

$$NDVI = \frac{(NIR - RED)}{(NIR + RED)} \quad (1)$$

$$NDVI_{season} = \sum_{month_n}^{month_{n+3}} NDVI \quad (2)$$

$$NDVI_{year} = \sum_{season_1}^{season_4} NDVI \quad (3)$$

Gap Filling with Linear Interpolation

The final step of preprocessing involved filling in temporal gaps in the data for each pixel. This was done by using a linear interpolation method to fill in gaps with the average of the images before and after a gap. The precedent December month and antecedent January month were removed from the final image collection after gap filling (Falanga Bolognesi *et al.* 2020; Gandhi 2021).

MLP Model

MLP models are a form of neural networks that use DL. They have shown promise in the field of remote sensing classification, specifically for classifying crop cover (Kussul *et al.* 2017). They perform well for nonlinear problems like forecasting nonlinear time series data (Tealab *et al.* 2017; Nosratabadi *et al.* 2021; Ahmed 2023).

The specific model used in this paper (Figure 4) is an open source MLP model made freely available through SciKit Learn (Pedregosa *et al.* 2011). SciKit Learn was selected as the primary framework for this classification model, although other frameworks such as PyTorch (Wu 2023) and TensorFlow (Yao *et al.* 2017) have also shown promise in remote sensing applications. The primary motivation for the selection of SciKit Learn as a framework lies in its ease of use, relative simplicity, and ease of propagation across a diverse selection of environments and hardware.

In this study, the ANN MLP model had one input layer, one hidden layer, and one output layer. This architecture was found to be optimal for extrapolating the model to an independent validation year. The input layer was sized in correspondence with the number of bands of the input image. For an input image containing 12 months of data, with each month containing six spectral bands along with a computed NDVI band, this was 84 (7 × 12 = 84) input bands, in addition to four seasonal NDVI sums and one annual NDVI sum, for a grand total of 89 input bands. The hidden layer size was selected via a grid-search hyperparameter optimization (detailed in "Architecture and Optimization"). The output layer was sized in accordance with the number of crop classes to be predicted, which in this study was five.

The model was developed using HLSL30 data for the year 2021 (January–December 2021) and validated based on HLSL30 data for the year 2022 (January–December 2022). Testing the model on a different year allowed us to assess its interannual transferability, as done by Maleki *et al.* (2023) and Teke (2022).

Architecture and Optimization

Parameter optimization for the MLP model used in this study was performed via grid search. This process involves dividing the parameter space into intervals and testing each combination of parameter values. The specific parameters optimized included the number of hidden layers, size of hidden layers, median number of training iterations, activation function, solver function, alpha value, and learning rate (constant, adaptive, or inverse scaling). The parameter options and ranges used in the grid search are detailed in Table 3.

The grid search evaluated a total of 11,340 models, the product of the number of options for each parameter. For each combination of parameters, the model was trained and evaluated based on accuracy. The optimal parameters, which resulted in the highest accuracy, are

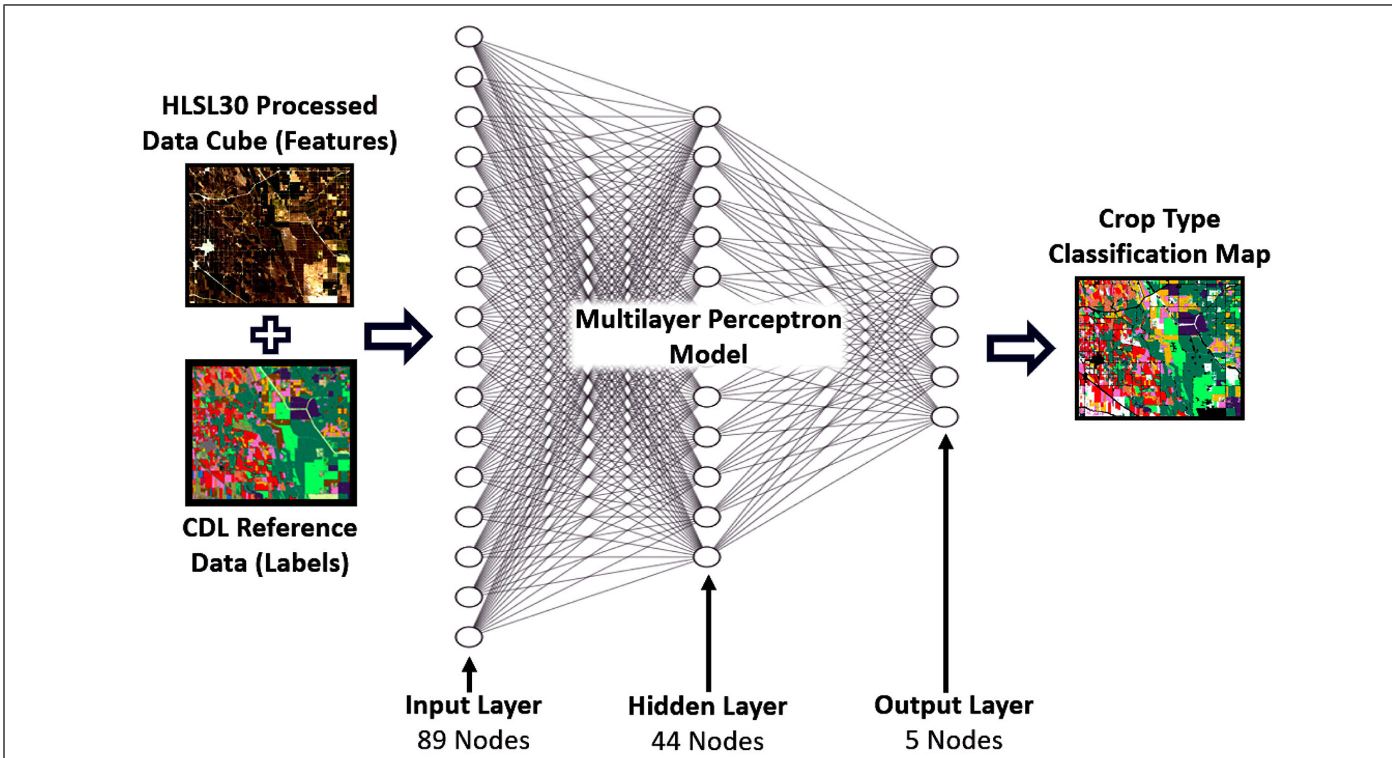

Figure 4. Multi-layer perceptron (MLP) architecture. The number of nodes in the input layer corresponds to the Harmonized Landsat 8 Sentinel-2 (HLS) Landsat 30-m (L30) 89-band data cube for the year 2021. The reference data on crop type classes (cotton, alfalfa, tree crops, grapes, and other) were obtained from the US Department of Agriculture (USDA) National Agricultural Statistics Service (NASS) Cropland Data Layer (CDL) for the year 2021 (USDA NASS 2022b). The hidden layer was approximately half the size of the input layer. The output layer corresponds to the number of crop classes being predicted using the Artificial Neural Network MLP model.

displayed in Table 4. Parameter optimization was performed on the USGS supercomputer Tallgrass (Falgout *et al.* 2024).

Accuracy varied from 51% to 74% across different runs, and processing time ranged from less than one minute to approximately 45 minutes for each run, depending on specific parameter values.

Model performance was evaluated via error matrices and the tabulation of Type 1 and Type 2 errors (errors of commission and omission respectively) (Teke 2022). User's accuracy was calculated as 100% − commission error, where commission error represents false-positive rates in classifying a certain class (e.g., a class other than cotton being classified as cotton). Producer's accuracy was similarly calculated as 100% − omission error, where omission error represents false-negative rates in classifying a certain class (e.g., cotton being misclassified as another class).

Table 3. Parameter space for grid search optimization.

Parameter Name	Options
Number of hidden layers	1, 2, 3
Hidden layer size	$\left[\frac{1}{2}\text{\#InputBands}\right]$, #InputBands, #InputBands*2
Maximum number of iterations	5, 10, 25, 50, 100, 150, 250
Activation function	tanh, relu, identity, logistic
Solver function	sgd, adam, lbfgs
Alpha value	0.00001, 0.0001, 0.001, 0.01, 0.1
Learning rate	constant, adaptive, invscaling

Table 4. Optimized parameters for final MLP model.

Parameter Name	Optimized Value
Number of hidden layers	1
Hidden layer size	$\left[\frac{1}{2}\text{\#InputBands}\right]$
Maximum number of iterations	100
Activation function	Rectified linear activation (relu)
Solver function	Adaptive moment estimation (adam)
Alpha value	0.0001
Learning rate	Constant

Results

Before applying the ANN MLP model, it was important to develop the knowledge base to understand class separability. To achieve this, we plotted the monthly average NDVI profiles of the five crop classes (cotton, alfalfa, tree crops, grapes, and other) that showed distinct separability of crop classes (Figure 5). Cotton had the most distinct NDVI profile, peaking in the summer months at nearly 0.8. Tree crops such as almonds and pistachios remained relatively constant throughout the year, with pistachios tending to have lower NDVI because of their young age and lack of ground cover. Grapes cyclically increased their NDVI in the warmer months and decreased in the cooler months. Alfalfa remained relatively constant throughout the year.

When a large number of bands like 89 are fed into ANN MLP (Figure 1) and trained with reference USDA CDL data to separate classes, the process goes through the generation of hidden layers, output layers, and finally a crop type classification map (Figure 1). First, we used the year 2021 HLSL30 data of 89 bands, trained them using USDA CDL, and ran the ANN MLP model to obtain the year 2021 crop type classification map. Initially, more than five crops were run, but the best accuracies were achieved when five classes were used that we could accurately replicate in other independent years.

Table 5. Classification error matrix. The counts for each category represent the number of 30×30-m pixel samples in the classified image.

	Cotton	Alfalfa	Grapes	Tree Crops	Other	Total	UA
Cotton	**75 168**	692	44	1545	9853	87 302	86%
Alfalfa	642	**43 446**	475	7192	12 080	63 835	68%
Grapes	111	3154	**26 737**	3393	2448	35 843	75%
Tree Crops	3339	2742	3886	**248 388**	55 325	313 680	79%
Other	6830	6060	897	82 766	**176 157**	272 710	65%
Total	86 090	56 094	32 039	343 284	255 863	**773 370**	
PA	87%	77%	83%	72%	69%	**OA =**	**74%**

OA = overall accuracy; PA = producer's accuracy; UA = user's accuracy.

Once a robust model was achieved, it was applied for the independent year 2022 to generate a crop type map for that year (Figure 6, right), to be compared with reference data from USDA CDL of the same year (Figure 6, left). As the results show, there is an excellent match between the ANN MLP–produced crop type map and its reference map. The error matrix (Table 5) shows producer's accuracies of the five classes varied between 69% and 87% (errors of omission: 13% and 31%). Cotton was captured the best, with 87% (missing 13%). The user's accuracies of the five classes varied between 65% and 86% (errors of commission: 14%–35%). Again, cotton was captured the best, with 86% (errors of commission: 14%). The overall classification accuracy was 74%. The greatest uncertainties were for the "other" class, which represents many land use/land cover classes.

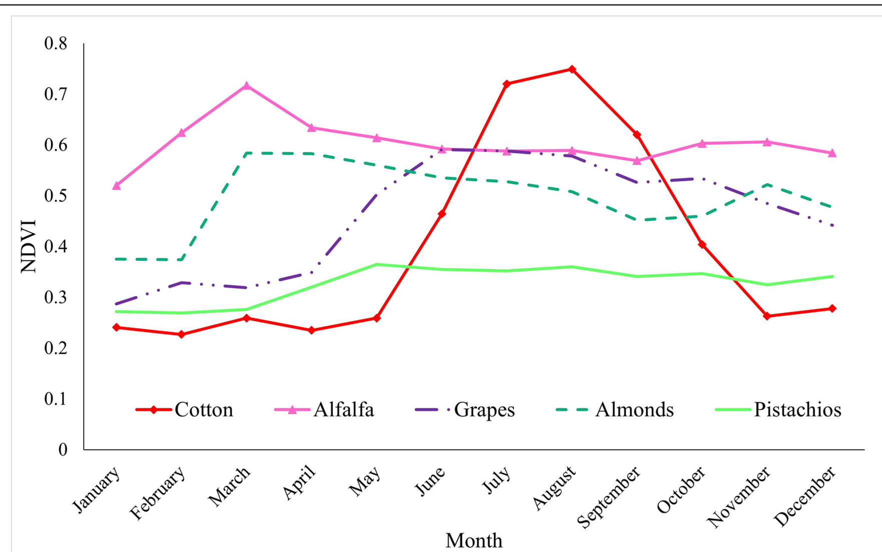

Figure 5. Average monthly Normalized Difference Vegetation Index (NDVI) time series by crop class for the year 2021.

The cotton class had the highest producer's and user's accuracies of all classes. This is because cotton, as an annual crop, has a clear phenological growth cycle so key in developing a temporal data–based model as seen in Figure 5. Its high canopy cover in the growing season also resulted in low variability across the cotton samples because of little noise from the soil background. In contrast, alfalfa had fields in various cutting and growth stages at any given time because of differences in farmers' management practices. The tree crops were in various years of development with soil background signatures contributing to the spectral profiles. The grape biomass also varied depending upon how old the grape vineyard was.

Discussion

In this study, we applied an ANN MLP DL model to HLSL30 89-band data cube to classify five crop classes within a discrete study area in the CCV for the year 2022. We achieved an overall accuracy of 74%, producer's accuracies of 69%–87%, and user's accuracies of 65%–86%.

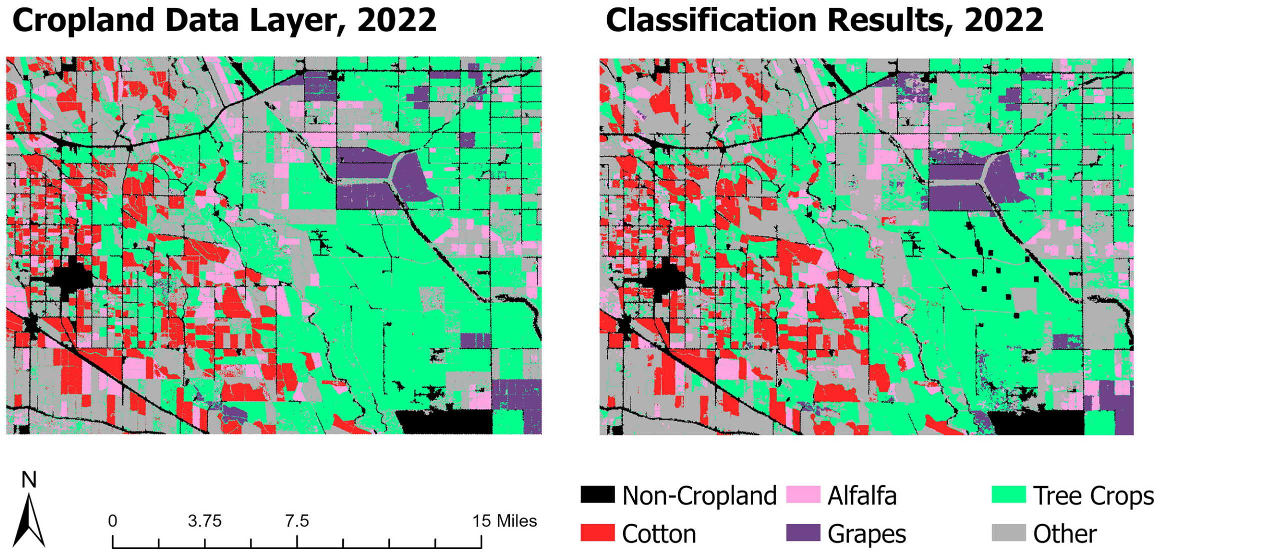

Figure 6. Final classification results, 2022. Using a multi-layer perceptron model trained on 2021 Harmonized Landsat 8 Sentinel-2 (HLS) Landsat 30-m (L30) data, five crop classes were classified with 74% accuracy. Non-Cropland area was masked prior to classification. The US Department of Agriculture (USDA) National Agricultural Statistics Service (NASS) Cropland Data Layer for 2022 (USDA NASS 2022b) is provided for comparison.

Several other studies have found MLP advantageous for crop type and land cover classification. He and Chen (2021) found several variations of MLP outperformed traditional ML and other DL classification algorithms in three case studies using hyperspectral remote sensing data to classify crop types and land cover classes, with overall accuracies of 87% to 94%. Wu *et al.* (2022) found similar results across four case studies, with overall accuracies of 92% to 99%. Karasu and Altan (2022) separated sesame crops from weeds with 98% overall accuracy using a combination of a convolutional neural network (CNN) model and MLP. Konduri *et al.* (2020) found accuracies as high as 90% when classifying crops within growing seasons in the United States, with higher accuracies coming from regions of lower crop type diversity. There are also many variations of MLP (Wu *et al.* 2022), including deep MLPs (Tripathi *et al.* 2022) and those using spectral and spatial information (He and Chen 2021), that may achieve higher classification accuracies. MLP Markov chains were successfully used to classify urban land use change over time with accuracies as high as 90% (Bendechou *et al.* 2024).

Although MLP models offer advantages in efficiency and predictive capability, they can have limitations, including overfitting and generalization challenges, the need for large volumes of training data (Moon *et al.* 2019), and long computation times for training with backpropagation (Bazrafshan *et al.* 2022). Maleki *et al.* (2023) found that although different years had similar climatic conditions, the timing of the crop phenological cycles varied by year, influencing model transferability and decreasing overall accuracy in the test years when using MLP as opposed to other DL models. Maleki *et al.* (2023) also found MLP was less robust to small sample sizes than some other models tested. For example, alfalfa is grown continuously within the CCV and is harvested as many as 10 times per year using staggered cutting cycles of 24–34 days (Orloff and Putnam 2006). This cycle introduces difficulty in time series analysis, as fields with the same crop will show drastically different spectral signatures if they are fully vegetated or recently harvested (Orloff and Putnam 2006).

Several studies have also used HLS data for crop type and land cover classification. For example, land cover and irrigated cropland classification analyses with HLS data resulted in overall accuracies of 90% (Falanga Bolognesi *et al.* 2020). Soybeans were classified using HLS data with overall accuracies of 91%. Hong *et al.* (2023) used HLS to classify land cover classes with an overall accuracy of 95%, with producer's and user's accuracy of 78% and 81% respectively for abandoned croplands. The 30-m spatial resolution of HLSL30 and HLSS30 data was successful for classifying rice cropping intensities in fragmented croplands in China (Hu *et al.* 2023). At the time of this study, the HLSS30 product was not available on GEE. However, the workflows developed in this study can easily be expanded to incorporate the HLSS30 product in GEE for future studies.

Apart from the spectral bands, we used NDVI because it is one of the most well-known and commonly used vegetation indices for phenological studies (Teke 2022; Hu *et al.* 2023). The Enhanced Vegetation Index is also common and avoids the issue of saturation at high levels of biomass, and may improve classification accuracies (Teke 2022; Hu *et al.* 2023). However, NDVI has been found to be robust to cross-year differences (Teke 2022) and can be more consistent across sensors and atmospheric correction methods (Hu *et al.* 2023). Li, Chen, *et al.* (2020) also used time series NDVI values for crop type classification in CCV. The consistently high NDVI values of alfalfa throughout the year were also found in Li, Chen, *et al.* (2020). As found in Li, Chen, *et al.* (2020), the NDVI for almonds and grapes in this study started off low in the winter and increased in the summer. The winter NDVI for both crop types was higher in our study area near Fresno compared with the northern Sacramento Valley in CCV, perhaps because of colder winters (Li, Chen, *et al.* 2020). Seasonal changes in pistachio NDVI values in this study are low, probably because the trees are still young with small canopies. Using several indices may further improve classification accuracies (Parreiras *et al.* 2022; Hong *et al.* 2023).

Other studies classifying crop types in CCV obtained varying levels of accuracy depending on the datasets and methods used. For example, Zhang *et al.* (2022) used Sentinel-2 and RF in GEE to map similar crops in CCV with high in-season classification accuracies. On the other hand, Konduri *et al.* (2020) found crop type classification in CCV challenging because of small fields, high crop type diversity, and the presence of many specialty crops, with an overall classification accuracy of 50%. This may be because the authors used coarser spatial resolution Moderate Resolution Imaging Spectroradiometer images and a cluster-then-label classification model (Konduri *et al.* 2020). Using RF and Synthetic Aperture Radar (SAR) data, Li, Zhang, *et al.* (2020) obtained overall classification accuracies of 85%–91% in their study area in CCV. Using CNN with Landsat 8 and Sentinel-2 data, Li, Chen, *et al.* (2020) obtained overall accuracies of 97%–99% in the CCV.

Although our study demonstrates the efficacy of MLP models, HLSL30 data, and NDVI time series in classifying crops in CCV, there are several avenues for further improving classification accuracies and advancing the field of remote sensing in agriculture. Incorporating additional spectral bands, such as those from hyperspectral sensors (He and Chen 2021; Wu *et al.* 2022; Wang *et al.* 2023), synthetic aperture radar sensors (Li, Zhang, *et al.* 2020; Maleki *et al.* 2023), or other phenological variables and vegetation indices (Teke 2022) could enhance discrimination between crop types. Moreover, integrating ancillary data sources, such as weather data or soil properties, may provide valuable context for classification models (Falanga Bolognesi *et al.* 2020; Yang *et al.* 2023). We used HLSL30 data and USDA NASS CDL data from 2021 and 2022 because they were the most recent years available at the time of analysis. Future work may expand to other years and areas of interest. Additionally, ongoing research into advanced ML techniques, including DL architectures and ensemble methods, holds promise for refining classification algorithms and achieving higher accuracies (Karasu and Altan 2022; Li, Chen, *et al.* 2020). The upcoming Landsat Next, with superspectral resolution along with Landsat's temporal and spatial resolutions, will further advance agricultural studies like this one.

Conclusion

This paper demonstrated the ability of the artificial neural network multi-layer perceptron (ANN MLP) deep learning (DL) model to classify agricultural crops using Harmonized Landsat 8 Sentinel-2 L-30 (HLSL30) time series data over a calendar year. A robust model developed in the study was applied to automatically classify five crop classes (cotton, alfalfa, tree crops, grapes, and other) in California's Central Valley (CCV) for an independent year with producer's accuracies of 69%–87% (errors of omission: 13%–31%) and user's accuracies of 65%–86% (errors of commission: 14%–35%). Cotton was captured the best with a producer's accuracy of 87% and user's accuracy of 86%. ANN MLP models are powerful tools for analyzing big data such as HLSL30 and HLS Sentinel 30m (HLSS30) data combined that are available every two to three days for the entire world to classify crops and support global food and water security studies and applications.

Acknowledgments

This research was supported by the US Geological Survey (USGS) National Land Imaging , Land Change Science, and Core Science Systems programs. The research was conducted in the science facilities of the USGS Western Geographic Science Center. Any use of trade, firm, or product names is for descriptive purposes only and does not imply endorsement by the US government. The authors thank the farmers who allowed us to visit their fields. The study data and results are described in McCormick *et al.* (2024).

References

Ahmed, S. 2023. A software framework for predicting the maize yield using modified multi-layer perceptron. *Sustainability* 15(4): 3017.

Aneece, I. and P. Thenkabail. 2022. New generation hyperspectral sensors DESIS and PRISMA provide improved agricultural crop classifications. *Photogrammetric Engineering and Remote Sensing* 88:715–729.

Bartels, R. J., A. W. Black and B. D. Keim. 2020. Trends in precipitation days in the United States. *International Journal of Climatology* 40(2):1038–1048.

Bazrafshan, O., M. Ehteram, Z. G. Moshizi and S. Jamshidi. 2022. Evaluation and uncertainty assessment of wheat yield prediction by multilayer perceptron model with bayesian and copula bayesian approaches. *Agricultural Water Management* 273:107881.

Bégué, A., L. Leroux, M. Soumaré, J.-F. Faure, A. A. Diouf, X. Augusseau, L. Touré and J.-P. Tonneau. 2020. Remote sensing products and services in support of agricultural public policies in Africa: Overview and challenges. *Frontiers in Sustainable Food Systems* 4:505081.

Bendechou, H., A. Akakba, K. M. Issam and H.A.B. Salem. 2024. Monitoring and predicting land use/land cover dynamics in Djelfa city, Algeria, using Google Earth Engine and a Multi Layer Perceptron Markov Chain model. *Geographica Pannonica* 28(1):1–20.

Cai, Y., K. Guan, J. Peng, S. Wang, C. Seifert, B. Wardlow and Z. Li. 2018. A high-performance and in-season classification system of field-level crop types using time-series Landsat data and a machine learning approach. *Remote Sensing of Environment* 210:35–47.

Cervantes, J., F. Garcia-Lamont, L. Rodríguez-Mazahua and A. Lopez. 2020. A comprehensive survey on support vector machine classification: Applications, challenges and trends. *Neurocomputing* 408:189–215.

Chen, Y., J. Hu, Z. Cai, J. Yang, W. Zhou, Q. Hu, C. Wang, L. You and B. Xu. 2024. A phenology-based vegetation index for improving ratoon rice mapping using Harmonized Landsat and Sentinel-2 data. *Journal of Integrative Agriculture* 23(4):1164–1178.

Claverie, M., J. Ju, J. Masek, J. Dungan, E. Vermote, J. Roger, S. Skakun and C. Justice. 2018. The Harmonized Landsat and Sentinel-2 surface reflectance data set. *Remote Sensing of Environment* 219:145–161.

Costa, W., L. Fonseca and T. Körting. 2015. Classifying grasslands and cultivated pastures in the Brazilian cerrado using support vector machines, multilayer perceptrons and autoencoders. In *Machine Learning and Data Mining in Pattern Recognition*, edited by P. Perner. Cham, Switzerland: Springer International Publishing, pp. 187–198.

DelSole, T., L. Trenary, Tippett, M. K., and K. Pegion. 2017. Predictability of week-3–4 average temperature and precipitation over the contiguous United States. *Journal of Climate* 30(10):3499–3512.

Falanga Bolognesi, S., E. Pasolli, O. R. Belfiore, C. De Michele and G. D'Urso. 2020. Harmonized Landsat 8 and Sentinel-2 time series data to detect irrigated areas: An application in southern Italy. *Remote Sensing* 12(8):1275. https://doi.org/10.3390/rs12081275.

Falgout, J. T., J. Gordon and M. J. Davis. 2024. USGS Advanced Research Computing, USGS Tallgrass Supercomputer. US Geological Survey. https://doi.org/10.5066/P9XE7ROJ.

Foley, D., P. Thenkabail, A. Oliphant, I. Aneece and P. Teluguntla. 2023. Crop water productivity from cloud-based Landsat helps assess California's gap-filling with linear interpolation. *Remote Sensing* 15(19):4894. https://doi.org/10.3390/rs15194894.

Gandhi, U. 2021. Temporal Gap-Filling with Linear Interpolation in GEE. <https://spatialthoughts.com/2021/11/08/temporal-interpolation-gee/>, archived at <https://web.archive.org/web/20240603231059/https://spatialthoughts.com/2021/11/08/temporal-interpolation-gee/> (last date accessed: 2 July 2024).

Gao, F., M. C. Anderson, D. M. Johnson, R. Seffrin, B. Wardlow, A. Suyker, C. Diao and D. M. Browning. 2021. Towards routine mapping of crop emergence within the season using the Harmonized Landsat and Sentinel-2 dataset. *Remote Sensing* 13(24):5074. https://doi.org/10.3390/rs13245074.

Gorelick, N., M. Hancher, M. Dixon, S. Ilyushchenko, D. Thau and R. Moore. 2017. Google Earth Engine: Planetary-scale geospatial analysis for everyone. *Remote Sensing of Environment* 202:18–27.

Gumma, M., P. Thenkabail, P. Panjala, P. Teluguntla, Takashi Yamano and I. Mohammed. 2022. Multiple agricultural cropland products of South Asia developed using Landsat-8 30 m and MODIS 250 m data using machine learning on the Google Earth Engine (GEE) cloud and spectral matching techniques (SMTs) in support of food and water security. *GIScience & Remote Sensing* 59(1):1048–1077.

He, X. and Y. Chen. 2021. Modifications of the multi-layer perceptron for hyperspectral image classification. *Remote Sensing* 13(17):3547. https://doi.org/10.3390/rs13173547.

Hong, C., A. V. Prishchepov, X. Jin, B. Han, J. Lin, J. Liu, J. Ren and Y. Zhou. 2023. The role of harmonized Landsat Sentinel-2 (HLS) products to reveal multiple trajectories and determinants of cropland abandonment in subtropical mountainous areas. *Journal of Environmental Management* 336:117621.

Hu, J., Y. Chen, Z. Cai, H. Wei, X. Zhang, W. Zhou, C. Wang, L. You and B. Xu. 2023. Mapping diverse paddy rice cropping patterns in South China using Harmonized Landsat and Sentinel-2 data. *Remote Sensing* 15(4):1034. https://doi.org/10.3390/rs15041034.

Inocente, G., D. Garbuglio and P. Ruas. 2022. Multilayer perceptron applied to genotypes classification in diallel studies. *Scientia Agricola* 79(3). https://doi.org/10.1590/1678-992X-2020-0365.

Kang, J., H. Zhang, H. Yang and L. Zhang. 2018. Support vector machine classification of crop lands using Sentinel-2 imagery, *2018 7th International Conference on Agro-geoinformatics (Agro-geoinformatics)*, 6–9 August 2018, Hangzhou, China (IEEE), pp. 1–6. doi: 10.1109/Agro-Geoinformatics.2018.8476101

Karasu, S. and A. Altan. 2022. Agricultural crop classification with R-CNN and machine learning methods, *International Mediterranean Congress*, 16–18 November 2022, Mersin, Turkey (Publisher: Location), pp. 591–603.

Karthikeyan, L., I. Chawla and A. K. Mishra. 2020. A review of remote sensing applications in agriculture for food security: Crop growth and yield, irrigation, and crop losses. *Journal of Hydrology* 586:124905.

Khan, A., A. Vibhute, S. Mali and C. Patil. 2022. A systematic review on hyperspectral imaging technology with a machine and deep learning methodology for agricultural applications. *Ecological Informatics* 69(101678):1–12.

Khanal, S., K. KC, J. P. Fulton, S. Shearer and E. Ozkan. 2020. Remote sensing in agriculture—Accomplishments, limitations, and opportunities. *Remote Sensing* 12(22):3783. https://doi.org/10.3390/rs12223783.

Konduri, V. S., J. Kumar, W. W. Hargrove, F. M. Hoffman and A. R. Ganguly. 2020. Mapping crops within the growing season across the United States. *Remote Sensing of Environment* 251:112048.

Kussul, N., M. Lavreniuk, S. Skakun and A. Shelestov. 2017. Deep learning classification of land cover and crop types using remote sensing data. *IEEE Geoscience and Remote Sensing Letters* 14(5):778–782.

Li, Z., G. Chen and T. Zhang. 2020. A CNN-transformer hybrid approach for crop classification using multitemporal multisensor images. *IEEE Journal of Selected Topics in Applied Earth Observations and Remote Sensing* 13:847–858.

Li, H., C. Zhang, S. Zhang and P. M. Atkinson. 2020. Crop classification from full-year fully-polarimetric L-band UAVSAR time-series using the random forest algorithm. *International Journal of Applied Earth Observation and Geoinformation* 87:102032.

Lu, B., Y. He and P. D. Dao. 2019. Comparing the performance of multispectral and hyperspectral images for estimating vegetation properties. *IEEE Journal of Selected Topics in Applied Earth Observations and Remote Sensing* 12:1784–1797.

Maleki, S., N. Baghdadi, C. F. Dantas, S. Najem, H. Bazzi, N. P. Reluy, D. Ienco and M. Zribi. 2023. Artificial intelligence algorithms for rapeseed fields mapping using Sentinel-1 time series: Temporal transfer scenario and ground sampling constraints. *IEEE Journal of Selected Topics in Applied Earth Observations and Remote Sensing* 16:8884–8899.

Martos, V., A. Ahmad, P. Cartujo and J. Ordoñez. 2021. Ensuring agricultural sustainability through remote sensing in the era of agriculture 5.0. *Applied Sciences* 11(13):5911. https://doi.org/10.3390/app11135911.

Masek, J., J. Ju, J. Roger, S. Skakun, E. Vermote, M. Claverie, J. Dungan, Z. Yin, B. Freitag and C. Justice. 2021. HLS operational land imager surface reflectance and TOA brightness daily global 30m v2.0 [data set]. NASA EOSDIS Land Processes Distributed Active Archive Center. <URL> Accessed 22 May 2024.

Masek, J., J. Ju, J.-C. Roger, S. Skakun, M. Claverie and J. Dungan. 2018. Harmonized Landsat/Sentinel-2 products for land monitoring, *IGARSS 2018—2018 IEEE International Geoscience and Remote Sensing Symposium*, 22–27 July 2018, Valencia, Spain (IEEE), pp. 8163–8165.

McCormick, R., I. Aneece, P. Thenkabail, A. Oliphant, P. Teluguntla and D. Foley. 2024. ANN-Classified Crop Type Map for the Year 2022 in California's Central Valley. U.S.G.S. ScienceBase Data Catalog. https://doi.org/10.5066/P19QFRTX.

Miller, G. J., J. T. Morris and C. Wang. 2019. Estimating aboveground biomass and its spatial distribution in coastal wetlands utilizing Planet multispectral imagery. *Remote Sensing* 11(17):2020. https://doi.org/10.3390/rs11172020.

Moon, T., S. Hong, H. Y. Choi, D. H. Jung, S. H. Chang and J. E. Son. 2019. Interpolation of greenhouse environment data using multilayer perceptron. *Computers and Electronics in Agriculture* 166:105023.

Nosratabadi, S., S. Ardabili, Z. Lakner, C. Mako and A. Mosavi. 2021. Prediction of food production using machine learning algorithms of multilayer perceptron and ANFIS. *Agriculture* 11(5):408. https://doi.org/10.3390/agriculture11050408.

Oliphant, A. J., P. S. Thenkabail, P. Teluguntla, J. Xiong, M. K. Gumma, R. G. Congalton and K. Yadav. 2019. Mapping cropland extent of Southeast and Northeast Asia using multi-year time-series Landsat 30-m data using a random forest classifier on the Google Earth Engine Cloud. *International Journal of Applied Earth Observation and Geoinformation* 81:110–124.

Orloff, S. and D. Putnam. 2006. Cutting schedule strategies to maximize returns. In *Proceedings of the 36th California Alfalfa & Forage Symposium*, 11-13 December 2006, Reno, Nevada (University of California Cooperative Extension, Department of Plant Sciences, University of California, Davis: Davis, California), pp. 11–13.

Ozdogan, M., Y. Yang, G. Allez and C. Cervantes. 2010. Remote sensing of irrigated agriculture: Opportunities and challenges. *Remote Sensing* 2(9):2274–2304.

Parreiras, T. C., É. L. Bolfe, M.E.D. Chaves, I. D. Sanches, E. E. Sano, D.d.C. Victoria, G. M. Bettiol and L. E. Vicente. 2022. Hierarchical classification of soybean in the Brazilian savanna based on Harmonized Landsat Sentinel data. *Remote Sensing* 14(15):3736.

Pedregosa, F., G. Varoquaux, A. Gramfort, V. Michel, B. Thirion, O. Grisel, M. Blondel, P. Prettenhofer, R. Weiss, V. Dubourg, J. Vanderplas, A. Passos, D. Cournapeau, M. Brucher, M. Perrot and E. Duchesnay. 2011. Scikit-learn: Machine learning in Python. *Journal of Machine Learning Research* 12:2825–2830.

Shen, L., J. B. Li, R. Wheate, J. Yin and S. S. Paul. 2020. Multi-layer perceptron neural network and Markov chain based geospatial analysis of land use and land cover change. *Journal of Environmental Informatics Letters* 3(1). https://doi.org/10.3808/jeil.202000023

Tealab, A., H. Hefny and A. Badr. 2017. Forecasting of nonlinear time series using ANN. *Future Computing and Informatics Journal* 2(1):39–47.

Teke, M. 2022. *Multi-year Time Series Crop Mapping.* Ph.D. thesis, Middle East Technical University, Ankara, Turkey, 119 p.

Teluguntla, P., P. Thenkabail, A. Oliphant, M. Gumma, I. Aneece, D. Foley and R. McCormick. 2023. *Landsat-Derived Global Rainfed and Irrigated-Cropland Product 30 m.* Version 001. Landsat-8. Location: NASA EOSDIS Land Processes Distributed Active Archive Center. URL

Teluguntla, P., P. Thenkabail, A. Oliphant, J. Xiong, M. Gumma, R. Congalton, K. Yadav and A. Huete. 2018. A 30-m Landsat-derived cropland extent product of Australia and China using random forest machine learning algorithm on Google Earth Engine cloud computing platform. *ISPRS Journal of Photogrammetry and Remote Sensing* 144:325–340.

Thenkabail, P., I. Aneece, P. Teluguntla and A. Oliphant. 2021. Hyperspectral narrowband data propel gigantic leap in the Earth remote sensing. *Photogrammetric Engineering & Remote Sensing* 87(7):461–467.

Thenkabail, P., P. Teluguntla, J. Xiong, A. Oliphant, R. Congalton, M. Ozdogan, M. Gumma, J. Tilton, C. Giri, C. Milesi, A. Phalke, R. Massey, K. Yadav, T. Sankey, Y. Zhong, I. Aneece and D. Foley. 2021. *Global Cropland-Extent Product at 30-m Resolution (GCEP30) Derived from Landsat Satellite Time-Series Data for the Year 2015 Using Multiple Machine-Learning Algorithms on Google Earth Engine Cloud. U.S. Geological Survey Professional Paper 1868*. Reston, Virginia: U.S. Geological Survey, 63 p.

Tripathi, A., R. K. Tiwari and S. P. Tiwari. 2022. A deep learning multi-layer perceptron and remote sensing approach for soil health based crop yield estimation. *International Journal of Applied Earth Observation and Geoinformation* 113:102959.

Tucker, C. J. 1979. Red and photographic infrared linear combinations for monitoring vegetation. *Remote Sensing of Environment* 8(2):127–150.

USDA NASS. 2022a. *2021 California Cropland Data Layer—NASS/USDA, Technical report, United States Department of Agriculture, National Agricultural Statistics Service.* <https://www.nass.usda.gov/> (last date accessed: 20 February 2024).

USDA NASS. 2022b. *Cropland Data Layer: NASS/USDA Metadata.* <https://www.nass.usda.gov/> (last date accessed: 9 June 2022).

Valero, S., D. Morin, J. Inglada, G. Sepulcre, M. Arias, O. Hagolle, G. Dedieu, S. Bontemps, P. Defourny and B. Koetz. 2016. Production of a dynamic cropland mask by processing remote sensing image series at high temporal and spatial resolutions. *Remote Sensing* 8(1):55. https://doi.org/10.3390/rs8010055.

Visher, S. S. 1954. *Climatic Atlas of the United States*. Harvard University Press: Cambridge Massachusetts, 415 p.

Wang, S., K. Guan, C. Zhang, Q. Zhou, S. Wang, X. Wu, C. Jiang, B. Peng, W. Mei, K. Li, Z. Li, Y. Yang, W. Zhou, Y. Huang and Z. Ma. 2023. Cross-scale sensing of field-level crop residue cover: Integrating field photos, airborne hyperspectral imaging, and satellite data. *Remote Sensing of Environment* 285:113366.

Wu, H., H. Zhou, A. Wang and Y. Iwahori. 2022. Precise crop classification of hyperspectral images using multi-branch feature fusion and dilation-based MLP. *Remote Sensing* 14(11):2713. https://doi.org/10.3390/rs14112713.

Wu, X. (2023). Building semantic segmentation of high-resolution remote sensing image buildings based on U-net network model based on Pytorch framework. In *2023 International Conference on Intelligent Supercomputing and BioPharma (ISBP)*, 6–8 January 2023, Zhuhai, China (IEEE), pp. 24–28. https://doi.org/10.1109/ISBP57705.2023.1006130910.1109/ISBP57705.2023.10061309.

Wulder, M. A., D. P. Roy, V. C. Radeloff, T. R. Loveland, M. C. Anderson, D. M. Johnson, S. Healey, Z. Zhu, T. A. Scambos, N. Pahlevan, M. Hansen, N. Gorelick, C. J. Crawford, J. G. Masek, T. Hermosilla, J. C. White, A. S. Belward, C. Schaaf, C. E. Woodcock, J. L. Huntington, L. Lymburner, P. Hostert, F. Gao, A. Lyapustin, J.-F. Pekel, P. Strobl and B. D. Cook. 2022. Fifty years of Landsat science and impacts. *Remote Sensing of Environment* 280:113195.

Xiong, J., P. Thenkabail, J. Tilton, M. Gumma, P. Teluguntla, A. Oliphant, R. Congalton, K. Yadav and N. Gorelick. 2017. Nominal 30-m cropland extent map of continental Africa by integrating pixel-based and object-based algorithms using Sentinel-2 and Landsat-8 data on Google Earth Engine. *Remote Sensing* 9(10):1065.

Yang, Z., C. Diao and F. Gao. 2023. Towards scalable within-season crop mapping with phenology normalization and deep learning. *IEEE Journal of Selected Topics in Applied Earth Observations and Remote Sensing* 16:1390–1402.

Yao, Y., H. Liang, X. Li, J. Zhang and J. He. 2017. Sensing urban land-use patterns by integrating Google Tensorflow and scene-classification models. arXiv:1708.01580 [cs.CV]. https://doi.org/10.48550/arXiv.1708.01580.

Yu, H., B. Kong, Y. Hou, X. Xu, T. Chen and X. Liu. 2022. A critical review on applications of hyperspectral remote sensing in crop monitoring. *Experimental Agriculture* 58(e26):1–18.

Zhang, C., L. Di, L. Lin, H. Li, L. Guo, Z. Yang, E. G. Yu, Y. Di and A. Yang. 2022. Towards automation of in-season crop type mapping using spatiotemporal crop information and remote sensing data. *Agricultural Systems* 201:103462.

Zhu, T. 2020. Analysis on the applicability of the random forest. *Journal of Physics: Conference Series* 1607(1):012123.

Individual Tree Segmentation Using Deep Learning and Climbing Algorithm: A Method for Achieving High-precision Single-tree Segmentation in High-density Forests under Complex Environments

He Ma, Fangmin Zhang, Simin Chen, and Jinge Yu

Abstract

Accurate individual tree segmentation, which is important for forestry investigation, is still a difficult and challenging task. In this study, we developed a climbing algorithm and combined it with a deep learning model to extract forests and achieve individual tree segmentation using lidar point clouds. We tested the algorithm on mixed forests within complex environments scanned by unmanned aircraft system lidar in ecological restoration mining areas along the Yangtze River of China. Quantitative assessments of the segmentation results showed that the forest extraction achieved a kappa coefficient of 0.88, and the individual tree segmentation results achieved F-scores ranging from 0.86 to 1. The climbing algorithm successfully reduced false positives and false negatives with the increased crown overlapping and outperformed the widely used top-down region-growing point cloud segmentation method. The results indicate that the climbing algorithm proposed in this study will help solve the overlapped crown problem of tree segmentation under complex environments.

Introduction

Forest ecosystems are complex functional systems, occupying one-third of the Earth's land area (Schiefer *et al.* 2020). As the largest carbon reservoir in terrestrial ecosystems, forests play a crucial role in maintaining the global carbon balance, significantly affecting future global climate stability and the development of human society (Torabzadeh *et al.* 2019). To accurately analyze the detailed conditions of global forests, efficient and accurate methods for forest inventory are urgently needed to effectively depict the detailed structure and current status of forests. Individual tree–based surveys, compared to regional statistical surveys, can more precisely obtain important parameters such as timber volume, biomass, and carbon storage, aiding in the accurate quantitative analysis of forests.

The key prerequisite for individual tree–based forest surveys is the high-precision extraction of individual trees. Only by accurately determining the information of individual trees in a forest can subsequent forest parameter extraction be performed. Therefore, the precise extraction of individual trees using remote sensing methods is essential for large-scale, detailed forest surveys, aiding in forest management and optimization. Lidar, as an emerging remote sensing technology, provides data with higher resolution and three-dimensional point cloud data, which can depict more detailed characteristics of individual trees and forest biomass (Li *et al.* 2015; Zhao *et al.* 2009). With technological advancements, airborne lidar scanning (ALS) increasingly provides extensive information on forest stands or tree characteristics (average tree height, tree count, and individual tree height) (Lovell *et al.* 2011), but it often lacks detailed information about the branch layer (Dassot *et al.* 2011). Additionally, compared to terrestrial lidar scanning (TLS), ALS typically has a lower point density, often limited to 10 points/m² (Lu *et al.* 2014). However, with the miniaturization of sensors and the rapid development of technologies related to unmanned aircraft systems (UAS), UAS lidar scanning (ULS) has achieved a point density that is 2 orders of magnitude higher than ALS (Kellner *et al.* 2019), making it feasible to extract individual tree information over large forest areas.

In the past two decades, individual tree segmentation algorithms have undergone rapid development. These methods can be roughly divided into two major categories (Zhen *et al.* 2016). The traditional category includes raster-based methods that use the canopy height model (CHM) as foundational data. In most case, CHM is selected to identify local maxima at tree-canopy tops and then delineate crown areas around the maxima by using methods such as variant of watershed segmentation (Wang *et al.* 2004), valley following (Gougeon 1995), edge detection (Koch *et al.* 2006), morphological reconstruction (Liu *et al.* 2016), or template matching (Pirotti 2010). However, existing studies have shown that CHM-based methods struggle to detect trees in the lower forest layers (Eysn *et al.* 2015). Moreover, broadleaf trees are predominantly asymmetrical in canopy form. The CHM approach produces poorer results when compared to methods that work directly from point clouds (Jaskierniak *et al.* 2015).

With technological innovation, more advanced tree detection techniques that operate directly on point clouds have been developed. One of the most well-known and commonly used methods is the top-down region-growing point cloud segmentation (PCS) method developed by Li *et al.* (2012). PCS achieved an overall accuracy of 94% in the Sierra National Forest, significantly surpassing traditional marker-controlled watershed segmentation (Tao *et al.* 2014). PCS has gradually become the mainstream individual tree segmentation method for ALS and ULS point cloud data. Despite this, PCS and other top-down segmentation methods have seen slow progress in improving accuracy.

He Ma, Fangmin Zhang and Jinge Yu are with the Collaborative Innovation Center on Forecast and Evaluation of Meteorological Disasters/Jiangsu Key Laboratory of Agricultural Meteorology, Nanjing University of Information Science and Technology, (fmin.zhang@nuist.edu.cn).

Simin Chen is with the School of Arts, Nanjing University of Information Science and Technology.

Corresponding author: Fangmin Zhang (fmin.zhang@nuist.edu.cn)

Received July 15, 2024, accepted October 17, 2024.

Photogrammetric Engineering & Remote Sensing
Vol. 91, No. 2, February 2025, pp. 101–110.
0099-1112/22/101–110

doi: 10.14358/PERS.24-00083R2

PEER-REVIEWED CONTENT
IS ONLY AVAILABLE TO
ASPRS MEMBERS AND SUBSCRIBERS

FOR MORE INFORMATION VISIT
MY.ASPRS.ORG

**PEER-REVIEWED CONTENT
IS ONLY AVAILABLE TO
ASPRS MEMBERS AND SUBSCRIBERS**

**FOR MORE INFORMATION VISIT
MY.ASPRS.ORG**

**PEER-REVIEWED CONTENT
IS ONLY AVAILABLE TO
ASPRS MEMBERS AND SUBSCRIBERS**

**FOR MORE INFORMATION VISIT
MY.ASPRS.ORG**

**PEER-REVIEWED CONTENT
IS ONLY AVAILABLE TO
ASPRS MEMBERS AND SUBSCRIBERS**

**FOR MORE INFORMATION VISIT
MY.ASPRS.ORG**

PEER-REVIEWED CONTENT
IS ONLY AVAILABLE TO
ASPRS MEMBERS AND SUBSCRIBERS

FOR MORE INFORMATION VISIT
MY.ASPRS.ORG

PEER-REVIEWED CONTENT
IS ONLY AVAILABLE TO
ASPRS MEMBERS AND SUBSCRIBERS

FOR MORE INFORMATION VISIT
MY.ASPRS.ORG

PEER-REVIEWED CONTENT
IS ONLY AVAILABLE TO
ASPRS MEMBERS AND SUBSCRIBERS

FOR MORE INFORMATION VISIT
MY.ASPRS.ORG

PEER-REVIEWED CONTENT
IS ONLY AVAILABLE TO
ASPRS MEMBERS AND SUBSCRIBERS

FOR MORE INFORMATION VISIT
MY.ASPRS.ORG

PEER-REVIEWED CONTENT
IS ONLY AVAILABLE TO
ASPRS MEMBERS AND SUBSCRIBERS

FOR MORE INFORMATION VISIT
MY.ASPRS.ORG

Lightweight Ship Object Detection Algorithm for Remote Sensing Images Based on Multi-scale Perception and Feature Enhancement

Wei Sun, Xinyi Shen, Xiaorui Zhang, and Fei Guan

Abstract

As global trade and maritime traffic develop, exploring ship detection in remote sensing images has become a research hotspot. However, ships in remote sensing images are so small that it leads to a high detection leakage rate and excessive model parameters, making them difficult to apply on remote sensing equipment with limited resources. To address the challenge, we propose a lightweight ship object detection algorithm, adaptive layered multi-scale You Only Look Once version 8 (ALM-YOLOv8), based on multi-scale perception and feature enhancement. To enhance the model's perception of contextual information in complex backgrounds, a multi-scale channel fusion module is constructed to extract features of various scales. To enhance the extracted features, a small-object detection layer and a dynamic channel attention convolution that assigns dynamic weights are proposed. Additionally, this study embeds the large separable kernel attention mechanism into the original network, which lightens the model. Experiments on the HRSC2016 dataset demonstrate the effectiveness of ALM-YOLOv8.

Introduction

Ships play a crucial role in global trade and transportation, as they undertake the majority of the tasks of transporting goods for international trade (Zhang *et al.* 2021; Kong *et al.* 2022). Over the past few years, with the development of satellite and drone technology, and the launch of a large number of remote sensing satellites, more and more studies have carried out relevant research on the detection of objects captured by remote sensing images (Wang, Li, *et al.* 2018; Chen *et al.* 2020). Especially when there are oil slicks and other marine pollution leaks, real-time monitoring of maritime ships through remote sensing images obtained from satellites or drones facilitates the rational planning of maritime resource development and use and the improvement of management efficiency of maritime shipping safety (Chen, Cui, *et al.* 2021).

Currently, detection of maritime ships quickly and accurately in remote sensing images has become a research hotspot (Sun *et al.* 2022). Initially, researchers used artificial features to detect ships (Huang *et al.* 2015; Leng *et al.* 2019; Chen, Xu, *et al.* 2021; Wang *et al.* 2021); preprocessing methods such as land and sea segmentation are often required to extract features with strong discriminatory power, but these methods have difficulties coping with the noise interference caused by complex background.

With the development of deep learning in the field of computer vision, object detection methods based on deep convolutional neural networks have demonstrated outstanding performance (Abbas *et al.* 2022). Some researchers have applied classical detection frameworks, such as Single Shot MultiBox Detector (SSD), Region-based Convolutional Neural Networks (R-CNN), and Faster Region-based Convolutional Neural Network (Faster R-CNN), to detect ship targets in real scenarios (Liu *et al.* 2016), and have proposed a series of improved models based on these detection frameworks (Wang, Wang, *et al.* 2018; Zhang *et al.* 2019). In order to improve the detection accuracy, these methods use different region proposal networks on feature maps of different resolution sizes, thereby improving detection accuracy and overall performance to some extent (Li *et al.* 2020). However, remote sensing images are acquired from a long distance and wide viewing angle, so they contains a large amount of background information, especially contextual information related to the detection of the ship target; for example, the ship is generally docked on the water at the shore of the harbor, as shown in Figure 1a. Traditional methods have limited receptive fields with respect to convolutional kernels, which makes it difficult to sense and fully use the contextual information in the background, such as water, shore, and harbor, thereby resulting in unsatisfactory detection effects. In addition, we can see in Figure 1b that ships occupy few pixels in remote sensing images, especially small ships that occupy even fewer pixels, which have fewer available features because of lacking sufficient appearance information. Traditional methods that use common standard convolution and a single extraction network not only fail to dynamically focus on target ships of different scales but also may lose some of the detailed features of ships in the downsampling process of multi-layer convolutions, especially for small target ships, with only a few features left. This leads to higher missed detection and false alarm rates. If one model can adaptively pay more attention to these small objects like human eyes during object detection, and fully excavate and exploit the most useful detail features, the accuracy and reliability of the model will be significantly improved in the detection of small ships.

To enhance the accuracy of ship detection in remote sensing images, most methods attempt to increase the number of branches of their networks. However, this inevitably entails complex network structures and numerous network parameters, which makes it difficult to transfer them to mobile devices such as satellites and drones. Additionally, the limited computing resources on satellites and drones make it difficult to achieve fast detection speed (Cheng *et al.* 2023). Although researchers have proposed many effective methods and techniques in decreasing model weight, including parameter pruning (Luo *et al.* 2017) and knowledge distillation (Hinton *et al.* 2015), these lightweight methods either directly eliminate the weights or channels of the network,

Wei Sun is with the School of Automation, Nanjing University of Information Science and Technology, Nanjing, 210044, Jiangsu, China, and the Jiangsu Collaborative Innovation Center on Atmospheric Environment and Equipment Technology, Nanjing, Nanjing, 210044, Jiangsu, China.

Xinyi Shen and Fei Guan are with the School of Automation, Nanjing University of Information Science and Technology, Nanjing, 210044, Jiangsu, China.

Xiaorui Zhang is with the College of Computer and Information Engineering, Nanjing Tech University, Nanjing, 211816, Jiangsu, China.

Corresponding author: Wei Sun (sunw0125@163.com)

Received July 22, 2024, accepted October 17 2024

Photogrammetric Engineering & Remote Sensing
Vol. 91, No. 2, February 2025, pp. 111–122.
0099-1112/22/111–122

doi: 10.14358/PERS.24-00085R2

PEER-REVIEWED CONTENT IS ONLY AVAILABLE TO ASPRS MEMBERS AND SUBSCRIBERS

FOR MORE INFORMATION VISIT MY.ASPRS.ORG

PEER-REVIEWED CONTENT
IS ONLY AVAILABLE TO
ASPRS MEMBERS AND SUBSCRIBERS

FOR MORE INFORMATION VISIT
MY.ASPRS.ORG

PEER-REVIEWED CONTENT
IS ONLY AVAILABLE TO
ASPRS MEMBERS AND SUBSCRIBERS

FOR MORE INFORMATION VISIT
MY.ASPRS.ORG

PEER-REVIEWED CONTENT
IS ONLY AVAILABLE TO
ASPRS MEMBERS AND SUBSCRIBERS

FOR MORE INFORMATION VISIT
MY.ASPRS.ORG

PEER-REVIEWED CONTENT
IS ONLY AVAILABLE TO
ASPRS MEMBERS AND SUBSCRIBERS

FOR MORE INFORMATION VISIT
MY.ASPRS.ORG

PEER-REVIEWED CONTENT
IS ONLY AVAILABLE TO
ASPRS MEMBERS AND SUBSCRIBERS

FOR MORE INFORMATION VISIT
MY.ASPRS.ORG

PEER-REVIEWED CONTENT
IS ONLY AVAILABLE TO
ASPRS MEMBERS AND SUBSCRIBERS

FOR MORE INFORMATION VISIT
MY.ASPRS.ORG

PEER-REVIEWED CONTENT
IS ONLY AVAILABLE TO
ASPRS MEMBERS AND SUBSCRIBERS

FOR MORE INFORMATION VISIT
MY.ASPRS.ORG

PEER-REVIEWED CONTENT
IS ONLY AVAILABLE TO
ASPRS MEMBERS AND SUBSCRIBERS

FOR MORE INFORMATION VISIT
MY.ASPRS.ORG

**PEER-REVIEWED CONTENT
IS ONLY AVAILABLE TO
ASPRS MEMBERS AND SUBSCRIBERS**

**FOR MORE INFORMATION VISIT
MY.ASPRS.ORG**

PEER-REVIEWED CONTENT
IS ONLY AVAILABLE TO
ASPRS MEMBERS AND SUBSCRIBERS

FOR MORE INFORMATION VISIT
MY.ASPRS.ORG

WHO'S WHO IN ASPRS

Founded in 1934, the American Society for Photogrammetry and Remote Sensing (ASPRS) is a scientific association serving thousands of professional members around the world. Our mission is to advance knowledge and improve understanding of mapping sciences to promote the responsible applications of photogrammetry, remote sensing, geographic information systems (GIS) and supporting technologies.

BOARD OF DIRECTORS

BOARD OFFICERS

President
Bandana Kar
U. S. Department of Energy (DOE)

President-Elect
Amr Abd-Elrahman
University of Florida

Vice President
Alvan Karlin, PhD, CMS-L, GISP
Dewberry

Past President
Lorraine B. Amenda, PLS, CP
Towill, Inc

Treasurer
John McCombs
NOAA

Secretary
Harold Rempel
ESP Associates, Inc.

COUNCIL OFFICERS

ASPRS has six councils. To learn more, visit https://www.asprs.org/Councils.html.

Sustaining Members Council
Chair: Paul Badr
Deputy Chair: Melissa Martin

Technical Division Directors Council
Chair: Hope Morgan
Deputy Chair: Tao Liu

Early-Career Professionals Council
Chair: Greg Stamnes

Region Officers Council
Chair: Demetrio Zourarakis
Deputy Chair: Cody Condron

Committee Chairs Council
Chair: David Day

Student Advisory Council
Chair: Oscar Duran
Deputy Chair: Ali Alruzuq

TECHNICAL DIVISION OFFICERS

ASPRS has seven professional divisions. To learn more, visit https://www.asprs.org/Divisions.html.

Geographic Information Systems Division
Director: Jin Lee
Assistant Director: Michael Baranowski

Lidar Division
Director: Matt Bethel
Assistant Director: Nora May

Photogrammetric Applications Division
Director: Hank Theiss
Assistant Director: Jae Sung Kim

Primary Data Acquisition Division
Director: Srini Dharmapuri
Assistant Director: Ravi Soneja

Professional Practice Division
Director: Hope Morgan
Assistant Director: Christian Stallings

Remote Sensing Applications Division
Director: Tao Liu
Assistant Director: Indu Jeyachandran

Unmanned Autonomous Systems (UAS)
Director: Bahram Salehi
Assistant Director: Rebecca Capps

REGION PRESIDENTS

ASPRS has 13 regions to serve the United States. To learn more, visit https://www.asprs.org/regions.html.

At Large
Hamdy Elsayed

Alaska Region
Caixia Wang

Cascadia Region
Jimmy Schulz

Eastern Great Lakes Region
Greg Lemke

Florida Region
Youssef Kaddoura

Gulf South
Scott Dunham

Heartland Region
Christian Stallings

Mid-South Region
Orrin Thomas

North Atlantic Region
Kurt Lutz

Northeast Region
Trevis Gigliotti

Pacific Southwest Region
Kris Taniguchi-Quan

Potomac Region
Trung Tran

Rocky Mountain Region
Melissa Martin

Western Great Lakes Region
Jason Krueger

SUSTAINING MEMBERS

Applanix
Richmond Hill, Ontario, Canada
http://www.applanix.com
Member Since: 7/1997

Ayres Associates
Madison, Wisconsin
www.AyresAssociates.com
Member Since: 1/1953

Dewberry
Fairfax, Virginia
www.dewberry.com
Member Since: 1/1985

Digital Mapping, Inc. (DMI)
Huntington Beach, California
www.admap.com
Member Since: 4/2002

Environmental Research Incorporated
Linden, Virginia
www.eri.us.com
Member Since: 8/2008

Esri
Redlands, California
www.esri.com
Member Since: /1987

GeoCue Group
Madison, Alabama
http://www.geocue.com
Member Since: 10/2003

GeoDyn GmbH
Munich, Germany
www.geodyn.com/index
Member Since: 3/2024

Geographic Imperatives LLC
Centennial, Colorado
Member Since: 12/2020

GPD Group
Columubs, Ohio
https://gpdgroup.com/
Member Since: 7/2024

GPI Geospatial Inc.
Orlando, Florida
www.aca-net.com
Member Since: 1/1994

Halff Associates, Inc.
Richardson, Texas
https://halff.com/
Member Since: 8/2020

Keystone Aerial Surveys, Inc.
Philadelphia, Pennsylvania
http://www.kasurveys.com
Member Since: 1/1985

Kucera International
Willoughby, Ohio
www.kucerainternational.com
Member Since: 1/1992

L3Harris Technologies
Broomfield, Colorado
www.l3harris.com
Member Since: 6/2008

Leica Geosystems AG
Heerbrugg, Switzerland
https://leica-geosystems.com/en-us/
Member Since: 1/1990

Merrick & Company
Greenwood Village, Colorado
www.merrick.com
Member Since: 4/1995

Miller Creek Associates
SeaTac Washington
www.mcamaps.com
Member Since: 12/2014

NV5 Geospatial
Sheboygan Falls, Wisconsin
www.quantumspatial.com
Member Since: 1/1974

PixElement
Belmont, Michigan
www.pixelement.com
Member Since: 2/2017

Riegl USA, Inc.
Orlando, Florida
https://www.rieglusa.com
Member Since: 11/2004

Sanborn Map Company
Colorado Springs, Colorado
www.sanborn.com
Member Since: 10/1984

Surdex Corporation
(a Bowman company)
Chesterfield, Missouri
www.surdex.com
Member Since: 12/2011

Surveying And Mapping, LLC (SAM)
Austin, Texas
www.sam.biz
Member Since: 12/2005

T3 Global Strategies, Inc.
Bridgeville, Pennsylvania
https://t3gs.com/
Member Since: 6/2020

Towill, Inc.
San Francisco, California
www.towill.com
Member Since: 1/1952

U.S. Dept. of Commerce/NOAA/NOS/ National Geodetic Survey
Chesapeake, Virginia
https://www.ngs.noaa.gov/
Member Since: 7/2009

U.S. Geological Survey
Reston, Virginia
https://www.usgs.gov/
Member Since: 4/2002

Vertical Mapping Resources
Reno, Nevada
www.verticalmapping.com
Member Since: 12/2024

Woolpert LLP
Dayton, Ohio
www.woolpert.com
Member Since: 1/1985

ASPRS SUSTAINING CORPORATE MEMBERSHIP

Join the leaders of the geospatial community

Sustaining Corporate membership in ASPRS helps your company serve your employees and customers.

With your membership, you serve your organization, but you also serve the greater geospatial profession and industry and you have a voice in controlling the future direction of ASPRS. Each Corporate Member of ASPRS has a seat on the Sustaining Corporate Members Council, which in turn has a seat on the ASPRS Board of Directors.

Your membership helps

- ASPRS set industry standards
- Provide continuing education and professional development
- Publish the PE&RS Journal with practical career-oriented articles as well as peer-reviewed research
- Publish technical books like the Manual of Remote Sensing
- Expand academic scholarships for students (your future customers and workforce)
- Provide networking and business development opportunities through our regional and national meetings
- Registration discount for all ASPRS Conferences
- Discount on all ASPRS Publications
- Individual employee savings on ASPRS membership
- Member benefits for 1 to 4 employees under your Sustaining Corporate Membership

ASPRS
CODE OF ETHICS

Honesty, justice, and courtesy form a moral philosophy which associated with mutual interest among people should be the principles on which ethics are founded.

Each person who is engaged in the use development and improvement of the mapping sciences (Photogrammetry Remote Sensing Geographic Information Systems and related disciplines) should accept those principles as a set of dynamic guides for conduct and a way of life rather than merely for passive observance. It is an inherent obligation to apply oneself to one's profession with all diligence and in so doing to be guided by this Code of Ethics.

Accordingly, each person in the mapping sciences profession shall have full regard for achieving excellence in the practice of the profession and the essentiality of maintaining the highest standards of ethical conduct in responsibilities and work for an employer all clients colleagues and associates and society at large and shall…

asprs THE IMAGING & GEOSPATIAL INFORMATION SOCIETY

www.asprs.org

1. Be guided in all professional activities by the highest standards and be a faithful trustee or agent in all matters for each client or employer.
2. At all times, function in such a manner as will bring credit and dignity to the mapping sciences profession.
3. Not compete unfairly with anyone who is engaged in the mapping sciences profession by:
   a. Advertising in a self-laudatory manner;
   b. Monetarily exploiting one's own or another's employment position;
   c. Publicly criticizing other persons working in or having an interest in the mapping sciences;
   d. Exercising undue influence or pressure or soliciting favors through offering monetary inducements.
4. Work to strengthen the profession of mapping sciences by:
   a. Personal effort directed toward improving personal skills and knowledge;
   b. Interchange of information and experience with other persons interested in and using a mapping science with other professions and with students and the public;
   c. Seeking to provide opportunities for professional development and advancement of persons working under his or her supervision;
   d. Promoting the principle of appropriate compensation for work done by person in their employ..
5. Undertake only such assignments in the use of mapping sciences for which one is qualified by education training and experience and employ or advise the employment of experts and specialists when and whenever clients' or employers' interests will be best served thereby.
6. Give appropriate credit to other persons and/or firms for their professional contributions.
7. Recognize the proprietary privacy legal and ethical interests and rights of others. This not only refers to the adoption of these principles in the general conduct of business and professional activities but also as they relate specifically to the appropriate and honest application of photogrammetry remote sensing geographic information systems and related spatial technologies. Subscribers to this code shall not condone promote advocate or tolerate any organization's or individual's use of these technologies in a manner that knowingly contributes to:
   a. deception through data alteration;
   b. circumvention of the law;
   c. transgression of reasonable and legitimate expectation of privacy.
8. Promote equity, inclusion and intellectual diversity in the mapping sciences. Encourage participation without regard to race, religion, gender, disability, age, national origin, political affiliation, sexual orientation, gender identity, or gender expression.

***PE&RS* READERSHIP HIGHLIGHTS**

ASPRS is in the Top 10!

In March, April, and May, 2024, *PE&RS* ranked 9th, 8th, and 9th, respectively, out of over 11,000 journals for full-text downloads with Ingenta Connect.

Circulation: 2,500

Total audience: 5,000*

Digital Edition Monthly Unique Views: 2,000+

Professional Demographics

Work Setting	% Composition
Corporate	30%
Academia	30%
Government	26%
Sole Proprietor	13%

Education	% Composition
Doctorate degree	32%
Post graduate degree	45%
4-year college degree	19%
2-year college degree	4%

ASPRS Certifications	Amount
ASPRS Certified Photogrammetrists	290+
ASPRS Certified Mapping Scientists†	130+
ASPRS Certified Technologists	40+

†Includes our new and fast-growing Lidar certification

*Based on 2 readers per copy as well as online views

Source: *PE&RS* Readership Survey, Summer 2023

PE&RS Media Kit 2025

asprs THE IMAGING & GEOSPATIAL INFORMATION SOCIETY

Founded in 1934, the American Society for Photogrammetry and Remote Sensing (ASPRS) is a scientific association serving professional members throughout the world. Our mission is to advance knowledge and improve understanding of mapping sciences to promote the responsible applications of photogrammetry, remote sensing, geographic information systems (GIS), and supporting technologies.

Our members are analysts/specialists, educators, engineers, managers/ administrators, manufacturers/ product developers, operators, technicians, trainees, marketers, and scientists/researchers. Employed in the disciplines of the mapping sciences, they work in the fields of Agriculture/Soils, Archeology, Biology, Cartography, Ecology, Environment, Forestry/ Range, Geodesy, Geography, Geology, Hydrology/Water Resources, Land Appraisal/ Real Estate, Medicine, Transportation, and Urban Planning/Development.

For more information, contact Bill Spilman at bill@innovativemediasolutions.com | (877) 878-3260 toll-free | (309) 483-6467 direct | (309) 483-2371 fax

Readership Habits

90%

of PE&RS readers have
10+ years experience
in their profession

89% of our readers agree that *PE&RS* is their

TRUSTED SOURCE

of information about their profession

---

3 out of **4**

PE&RS readers save their issues for future reference

70% of *PE&RS* readers select, authorize or approve the products of products and services

---

Time spent reading *PE&RS* (average)

45

minutes

Our readers are regular attendees of the ASPRS Annual Conference as well as:

Geo Week, Esri, URISA, SPAR/AEC, GEOINT, Commercial UAV Expo, AUVSI

	% Composition
Read regularly (at least 3 out of 4 monthly issues)	54%

Products and services used or purchased in past 12 months	
GPS	92%
Computer Workstations	52%
Lidar	50%
Unmanned Aerial Systems	45%
GIS	45%
Data Storage Devices	42%
Aerial Photography	35%
Cameras	35%
Terrain Modeling	30%

30%

of *PE&RS* readers have a geospatial information technology budget of

$1 million or greater

for the current fiscal year.

Source: *PE&RS* Readership Survey, Summer 2023

PE&RS 2025 Advertising Rates & Specs

THE MORE YOU ADVERTISE THE MORE YOU SAVE! PE&RS offers frequency discounts. Invest in a three-times per year advertising package and receive a 5% discount, six-times per year and receive a 10% discount, 12-times per year and receive a 15% discount off the cost of the package.

	Sustaining Member Exhibiting at a 2025 ASPRS Conference	**Sustaining Member**	**Exhibitor**	**Non Member**
All rates below are for four-color advertisments				
Cover 1	$1,850	$2,000	$2,350	$2,500
In addition to the cover image, the cover sponsor receives a half-page area to include a description of the cover (maximum 500 words). The cover sponsor also has the opportunity to write a highlight article for the journal. Highlight articles are scientific articles designed to appeal to a broad audience and are subject to editorial review before publishing.				
Cover 2	$1,500	$1,850	$2,000	$2,350
Cover 3	$1,500	$1,850	$2,000	$2,350
Cover 4	$1,850	$2,000	$2,350	$2,500
Advertorial	1 Complimentary Per Year	1 Complimentary Per Year	$2,150	$2,500
Full Page	$1,000	$1,175	$2,000	$2,350
2 page spread	$1,500	$1,800	$3,200	$3,600
2/3 Page	$1,100	$1,160	$1,450	$1,450
1/2 Page	$900	$960	$1,200	$1,200
1/3 Page	$800	$800	$1,000	$1,000
1/4 Page	$600	$600	$750	$750
1/6 Page	$400	$400	$500	$500
1/8 Page	$200	$200	$250	$250
Other Advertising Opportunities (see page 5 for full descriptions)				
Employment Promotion	$500 (30 day web + 1 email) $300 (30 day web)	$500 (30 day web + 1 email) $300 (30 day web)	$500 (30 day web + 1 email) $300 (30 day web)	$500 (30 day web + 1 email) $300 (30 day web)
Dedicated Content Email blast	$2,500	$2,500	$2,500	$2,500
Newsletter Display Advertising	1 Complimentary Per Year	1 Complimentary Per Year	$500	$500
PE&RS Announcement E-Mail	$1000	$1000	$1000	$1000

A 15% commission is allowed to recognized advertising agencies

Ad Size	**Width**	**Height**
Cover	8.625”	11.25”
Full Page	8.375”	10.875”
2/3 Page Horizontal	7.125”	6.25”
2/3 Page Vertical	4.58”	9.625”
1/2 Page Horizontal	7.125”	4.6875”
1/2 Page Vertical	3.4375”	9.625”
1/3 Page Horizontal	7.125”	3.125”
1/3 Page Vertical	2.29”	9.625”
1/4 Page Horizontal	7.125”	2.34”
1/4 Page Vertical	3.4375”	4.6875”
1/8 Page Horizontal	7.125”	1.17”
1/8 Page Vertical	1.71875”	4.6875”

Send ad materials to:
Rae Kelley (rkelley@asprs.org)

- Publication Size: 8.375” × 10.875” (W x H)
- Live area: 1/2” from gutter and 3/8” from all other edges
- Software Used: PC InDesign
- Supported formats: TIFF, EPS, BMP, JPEG, PDF, PNG PC InDesign, Illustrator, and Photoshop

For more information, contact Bill Spilman at bill@innovativemediasolutions.com | (877) 878-3260 toll-free | (309) 483-6467 direct | (309) 483-2371 fax

For more information, contact Bill Spilman at bill@innovativemediasolutions.com | (877) 878-3260 toll-free | (309) 483-6467 direct | (309) 483-2371 fax